Geotechnical characterization and seismic response of shallow geological formations in downtown Lisbon

Paula Teves-Costa[1,*], Isabel M. Almeida[2], Isabel Rodrigues[1], Rita Matildes[1,2], Claudia Pinto[2,3]

[1] *Instituto Dom Luiz, Faculdade de Ciências, Universidade de Lisboa, Lisboa, Portugal*

[2] *Centro de Geologia, Faculdade de Ciências, Universidade de Lisboa, Lisboa, Portugal*

[3] *Câmara Municipal de Lisboa, Campo Grande, Lisboa, Portugal*

Article history
Received August 5, 2013; accepted July 16, 2014.
Subject classification:
Site effects, Lisbon, Geotechnical database, Theoretical transfer functions, Ground motion amplification.

ABSTRACT

The geological and geotechnical characterization of shallow formations is one of the main steps in performing a microzonation study. This paper presents an example of the usefulness of the information compiled in a geological and geotechnical database for the estimation of the seismic response of the shallower formations of the Lisbon downtown area of Baixa. The geotechnical characterization of this area was performed based on the analysis of Standard Penetration Test (SPT) data compiled in the geological and geotechnical database. This database, connected to a geoscientific information system (CGIS), allows, also, the definition of 2D geological profiles used for estimating the thickness of the shallower layers. The shear-wave velocities (V_S) for each layer were estimated from empirical correlations using mean SPT values computed from the statistical evaluation of the compiled data. These V_S values were further calibrated with ambient vibration recording analysis. The seismic response of Baixa's superficial deposits was estimated by applying a 1D equivalent linear method to a set of soil profiles, regularly distributed across the area, and using synthetic accelerograms to simulate input motions associated with probable earthquake occurrences in Lisbon. The results are presented in terms of maps of predominant frequencies, with the corresponding amplification level, as well as spectral amplification factors for 1 Hz and 2.5 Hz. The results show that the fundamental frequency of the Baixa area is between 1.2 Hz and 2 Hz, for the whole central valley, reaching 3 Hz near the edges where anthroprogenic and alluvial deposits have less expression. Amplification factors up to 5 were obtained. These results were achieved regardless of the considered input motion. The similarity of the obtained fundamental frequency with the natural frequency of Baixa's old building stock increases the probability of resonance effects in future earthquakes.

1. Introduction

It is recognized that the characteristics of seismic ground motion can be locally modified due to the existence of soft surface layers or basin geometry [e.g., Bard and Bouchon 1985, Idriss 1990]. Examples may be found from several past earthquakes going back over several decades [e.g., Chavéz-García and Bard 1994, Bouckovalas and Kouretzis 2001, Duval et al. 2001, Giammarinaro et al. 2005, Fritsche et al. 2009, Navarro et al. 2009, Maugeri et al. 2011]. Several studies have shown the existence of resonance effects due to the coincidence of the natural period of the shallower soil layers and the fundamental period of buildings built on the soils resulting, often, in unexpectedly higher levels of damage [e.g., Bakir et al. 2002, Gallipoli et al. 2003, Mucciarelli et al. 2004, Gosar et al. 2010]. Consequently, the damage distribution observed during an earthquake can be conditioned by this effect, which can increase up to two degrees the observed EMS intensity (European Macroseismic Scale - EMS98; Grünthal [1998]). A paradigmatic example occurred during the 1985 Michoacán earthquake (Mexico). However, other examples can be found for more recent earthquakes occurring worldwide (e.g., Izmit, Turkey, 1999; Chi-Chi, Taiwan, 1999; Mula, Spain, 1999; Al Hoceimas, Morocco, 2004; Abruzzo, Italy, 2009), where the upper, normally consolidated soft deposits were responsible for an increase in the ground motion level for some specific periods [e.g., Navarro et al. 2000, Maugeri et al. 2011]. Therefore, the estimation of the seismic behavior of soils for a large town exhibiting moderate to high seismic risk, such as Lisbon, is of great importance for the damage assessment for a future earthquake.

During its history, Lisbon has been affected by several medium to strong earthquakes that caused considerable damage and produced large economic and social impacts. In particular, the very large and well known November 1st, 1755, earthquake (M ≥ 8) caused the complete destruction of its downtown area (Baixa), which was reconstructed with the application of the first implemented seismic resistant rules [Pereira de Sousa 1909, Cóias e Silva 2005]. Besides this kind of event, generated due to the slow collision of the Euroasiatic and the African tectonic plates, Lisbon can also be affected by earthquakes with moderate magnitudes and with epicenters located nearer to the city, such as the January 26, 1531, earthquake (M ≈ 7) generated inland in the Lower Tagus valley seismogenic zone [Moreira 1991].

Knowledge of the seismic response of the surface layers is fundamental for estimating the potential damage due to the occurrence of a medium to strong earthquake. The estimation of the soil fundamental frequencies and, if possible, the amplification of the ground motion during an earthquake, should be the main goal of microzonation studies conducted in urban areas [e.g., Fäh et al. 1997, Ansal et al. 2004, Giammarinaro et al. 2005, Anbazhagan and Sitharam 2008, Ansal et al. 2010]. Several methodologies can be applied to perform these kinds of studies but there is no consensus on the most effective procedure for estimating the seismic behavior of soils and the potential site amplification effects [Bard 1999, Mucciarelli and Gallipoli 2006].

In recent years, it has become common practice to classify soils into a small number of classes according to the V_{S30} value (average shear-wave velocity in the upper 30 m of the sub-surface), as presented in Eurocode 8 (EC8) [IPQ 2010], although any statistical test would conclude that this parameter has no (or a very weak) link to seismic amplification [Castellaro et al. 2008, Lee and Trifunac 2010]. Several authors proposed soil classifications that are not only based on code recommendations (V_{S30} values), but also use complementary information, usually F_0 (fundamental frequency) obtained from microtremor analysis [e.g., Luzi et al. 2011, Cadet et al. 2012]. However, both geotechnical engineers and seismologists agree that the site conditions can be estimated using the V_S profile down to bedrock.

Several geophysical techniques can be used for measuring S-wave velocities and to define the V_S profile. Some of these techniques could provide good quality results but they are not often used in microzonation studies because they are not easy to implement in an urban environment. Quick and cheap techniques have been developed using ambient vibration measurements. In particular, Nakamura's technique [Nakamura 1989, 1996, 2000], based on the interpretation of the horizontal-to-vertical spectral ratio (H/V) computed from ambient vibration records, has been widely used over recent decades in several cities worldwide [Lermo and Chávez-García 1994, Theodulidis and Bard 1995, Duval et al. 2001, Lebrun et al. 2001, Teves-Costa and Senos 2004, Tuladhar et al. 2004, Kamalian et al. 2008, Gosar et al. 2010, Fnais et al. 2014]. The theoretical basis of the method is controversial but the use of this technique to estimate site effects has been validated by comparison with both simulations and earthquake recordings [e.g., Bard et al. 1997, Bonnefoy-Claudet et al. 2006a, 2006b, Haghshenas et al. 2008].

Due to its seismic history, Lisbon has been the subject of several studies performed by different authors since the early 1990's, with the objective of estimating plausible seismic scenarios for the city. Oliveira [2008] presented an extensive review of the studies performed, pointing to the uncertainties and proposing the development of further work to reduce them. Also, several hazard studies were performed in the last few years for mainland Portugal and the Iberian Peninsula [Montilla et al. 2002, Sousa and Costa 2009, Vilanova et al. 2012] focusing mainly on the estimation of attenuation laws.

The seismic response of Lisbon's soils was also addressed in previous studies: Mendes-Victor et al. [1994] characterized the seismic behavior of soils by means of impedance contrast to bedrock; Teves-Costa et al. [1995] developed a map of dominant frequencies based on ambient vibration recordings analysis; Teves-Costa et al. [2001] performed a linear 1D theoretical analysis based on data presented in the geological map of Almeida [1986]. In the work developed for the Metropolitan Area of Lisbon, in 2001, the soil behavior was estimated by 1D non-linear analysis of specific soil profiles defined from geological and geotechnical logs. However, the work required was very large and the information provided for Lisbon was poorly detailed [Oliveira 2008].

Recently, as part of the Portuguese research project GeoSIS_Lx (http://geosislx.cm-lisboa.pt), new and old information on detailed the geology and geotechnical properties, based on down-hole information, were compiled and implemented in a geographical information system (GIS) [Almeida et al. 2010]. The main objective of this project was to allow the use of conventional geological information, as presented in the Lisbon geological map, together with engineering geological data obtained from site investigations, for a wide variety of applications. In particular, it was possible to perform geological and geotechnical 3D modelling of the city [Matildes et al. 2010].

The goal of this paper is to show the applicability of the geological and geotechnical database to microzonation studies, in particular on the geotechnical characterization of the shallower formations, as has been carried out in other countries with similar databases, e.g. in Spain [Cadet et al. 2011], Turkey [Hasancebi and

Ulusay 2006, Koçkar and Akgün 2007], India [Anbazhagan and Sitharam 2008, Maheswari et al. 2010b, Anbazhagan et al. 2013], Malaysia [Nabilah and Balendra 2012] and Iran [Akbari et al. 2011]. With this objective in mind, the geotechnical characterization of Baixa's shallow geological formations, based on Standard Penetration Test (SPT) data analysis, and the estimation of their seismic response, are presented. After providing a general geological and geomorphological framework of Lisbon and its downtown area - Baixa, the paper is structured as follows:

(i) a brief description of the geological and geotechnical modeling, obtained in the GeoSIS_Lx project using the database information [Matildes et al. 2010], enabling the identification of the physical properties of any soil profile (lithological description, thickness and depth to bedrock);

(ii) the statistical analysis of the Standard Penetration Test data contained in the database (N_{SPT} values), enabling the geotechnical characterization of three distinct zones in Baixa;

(iii) estimation of unit weight and V_S values for each layer, based on empirical relations using the analyzed NSPT data [e.g., Imai 1977, Lee 1990, Dikmen 2009];

(iv) calibration of the obtained V_S values using microtremor records;

(v) computation of a 1D soil response for a set of soil profiles regularly spaced using the equivalent linear model [Schnabel et al. 1972] and considering a set of near and far simulated earthquakes. Corresponding transfer functions were computed.

The results are presented in terms of maps of dominant frequencies and spectral amplification factors for the Baixa area.

2. Geological and geomorphological setting

Lisbon grew around an historical center which includes the downtown area (Baixa) (Figure 1). This area has been occupied since prehistorical times due to its strategic geographical location in relation to fluvial, estuarine and marine environments. Archaeological remains show a prehistory of early occupation in small settlements and a long, evolving urban occupation, since the mid-first millennium BC to the present.

In 1755, when Lisbon was struck by a major earthquake, Baixa was the most damaged area, not only due to the site response to the strong ground motion but also due to the tsunami that followed and the fire triggered by the earthquake. The almost total destruction of this area required major reconstruction leading to a new urban plan, with a geometric design. The new town was built over the ruins and, as a consequence of the great volume of debris, a thick layer of man-made (anthropogenic) materials, locally buried in the soft alluvial deposits, covered the creek area. Due to this process, the local coastline was artificially moved closer to its present-day location [Almeida et al. 2008].

The geological setting of Lisbon (Figure 1) is characterized by two geological environments. The SW area landscaped in Mesozoic formation materials in-

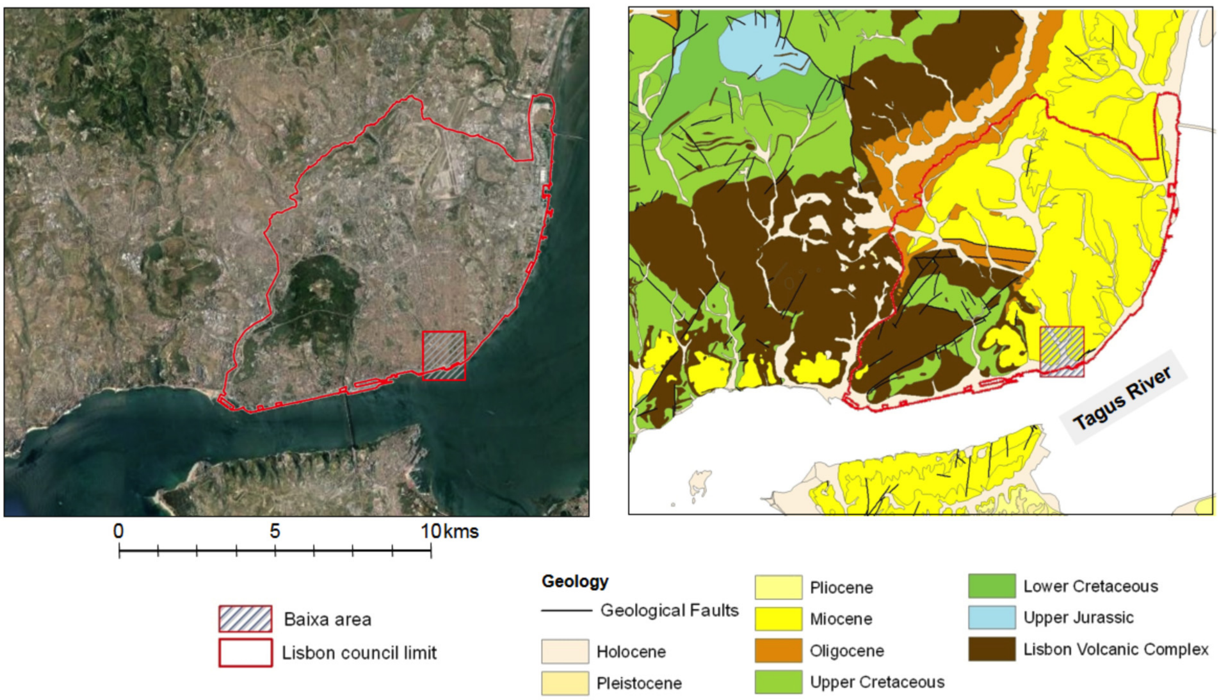

Figure 1. Location of the Lisbon City Council boundary and the Baixa area. Left: Aerial view from Google Earth. Right: Geological map of Lisbon and the surrounding area (adapted from the 1:100,000 Lisbon Metropolitan Area geological map).

cludes Cretaceous marls and limestones and neo-Cretaceous basalts. The E and NE area have Cenozoic formations, mainly Palaeocene and Miocene sedimentary series, associated with the genesis and evolution of the Tagus river basin. During the Miocene, an open connection with the sea allowed the deposition of a complete estuarine sequence, with alternating marine and continental facies. The thickness of the complete sequence can be as great as approximately 300 m. As the Miocene units form a monocline dipping east, the sequence becomes thicker eastwards. The Pliocene and Pleistocene sedimentation represents new conditions in the basin with a predominantly sandy sequence. The Holocene fluvial deposits are characterized by a sequence of sandy and clayey lenticular beds with lateral and vertical facies variations.

The Baixa area, located in the northern estuarine margin of the Tagus River, corresponds to the fluvial outlet of a 6.2 km^2 elongated basin cut in the Miocene bedrock [Almeida et al. 2009]. The valley is filled by a thick layer of alluvial sediments (normally consolidated silty sands and organic silty clays).

The Miocene formations present in the area correspond to the base of the Lisbon sequence defined by Cotter [1956] and characterized by alternating units with marine and continental influence and large vertical and lateral variations of facies. In the area, the Miocene sequence includes overconsolidated soils and soft rocks, gently tilted south and southeast with local undulations, giving rise to the geomorphologic setting with incised valleys bounding gentle hills. In this sequence, the different units, although very variable, are characterized by the main lithologies including (Figure 2): silty clayey soils and calcarenites (M_{Pr} and M_{FT}); fine micaceous sandy and silty sandy soils (M_{Es}, M_{QB} and M_{pm}); limestones, calcarenites and coquinites (M_{EC}, M_{CV} and M_{Mu}).

Located at the northern Tagus' margin, the Baixa area is morphologically marked by a depressed area between gentle hills (Figure 2). Affected by tides since historical times, the natural alluvial infill is almost completely covered by anthropogenic deposits.

3. Geotechnical characterization and 3D modelling

3.1. Geological and geotechnical modelling

As already mentioned, downtown Lisbon suffered a number of changes due to human interventions during its different phases of occupation and, also, severe damage caused by earthquakes. In recent decades, a large number of engineering works, especially for urban, subway and infrastructural development, were carried out. The amount of geological and geotechnical information produced constitutes an important contribution to the knowledge of the geology and the geotechnical characteristics of the area.

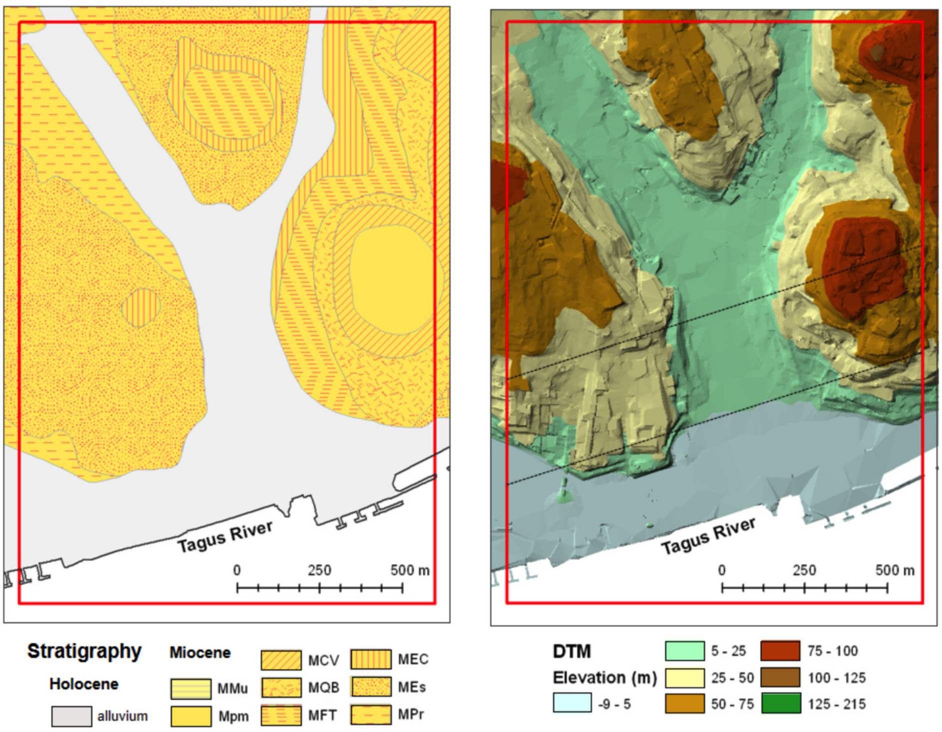

Figure 2. Left: Surface geology of the Baixa area (adapted from Pais et al. [2006]). The central part is filled by alluvial sediments covering Miocene formations (see lithological composition in the text). Right: Digital terrain model (DTM) obtained from a 1:1000 survey scale. Dashed black lines separate the three defined zones (north, central and south).

As part of the GeoSIS_Lx research project, a geotechnical and geological database has been developed to include *in situ* investigation data (borehole interpretation, sampling and geotechnical measurements) and laboratory test results. The database design follows a hierarchical data structure keeping subjective data interpretation to a minimum. Due to the lack of standard practices, it was also necessary to simplify and group the properties of some parameters to minimize their variability. The implementation of the GeoSIS_Lx geoscientific information system (CGIS) [Turner 2003] interactive with the database, allowed the storage of the information collected and made the data available for several purposes such as urban planning and engineering design [Almeida et al. 2010]. Currently, the database contains 924 site investigation reports, 5976 borehole logs and 38,560 N_{SPT} data. This geotechnical information is a secondary but important input for the 3D geological model and, once implemented, is also useful to cross validate the model.

The geological modeling was carried out based on the interpretation of the geological 1:10,000 scale map [Almeida 1986], the retrieval of database information and the automatic processing of such information with Matlab scripts. Considering the large volume of information and the uncertainty associated with existing data it was necessary, in a first iteration, to select the most trustworthy records purging more obvious errors. Using a small Matlab script on the spreadsheets it was possible to debug some information to produce a more consistent data set [Matildes et al. 2010]. The information included in the collected borehole profiles was considered in this processing, as well as the correspondence between stratigraphy, lithology and *in situ* tests (SPT). The registered data points were interpolated for the whole downtown Lisbon area, through a kriging algorithm, to determine the surfaces representing the lower boundary of each formation of interest.

Taking into account that anthropogenic deposits only appear at the top of the sequence, the thickness of surface materials was obtained by considering the digital terrain model surface and the base of the anthropogenic and alluvial deposits (Figure 3).

The data regarding anthropogenic deposits in all boreholes were used to model their thickness. A total of 666 borehole logs were used to interpolate the corresponding lower boundary surface. Considering the amount of urban development in the study area, it was assumed that anthropogenic deposits are constantly present although with variable thickness and significance (Figure 3).

For the alluvial deposits modeling, the logs of all boreholes that did not reach bedrock were discarded as they provided limited information on the thickness of the alluvium [Matildes et al. 2011]. The alluvium deposits basal surface was created by interpolation data

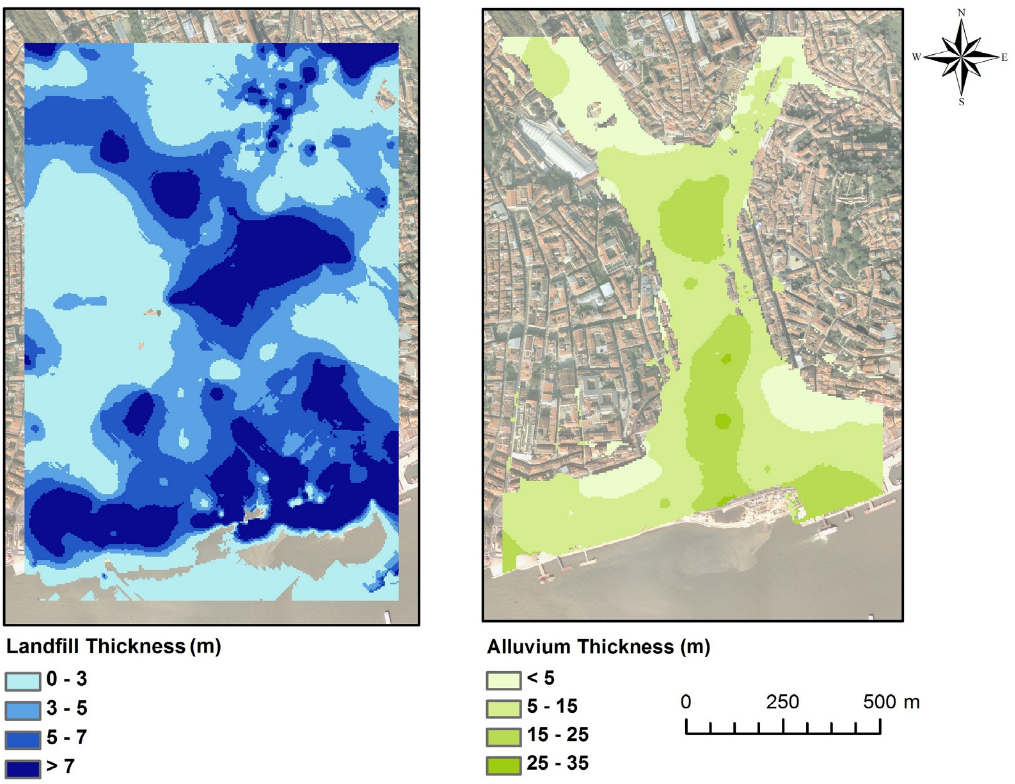

Figure 3. Thickness of anthropogenic deposits (left) and alluvial deposits (right) in Baixa.

from 442 borehole logs. The interpolation algorithm takes only into account the depth of the surface at each point and the output is a continuous surface in space, regardless of other parameters of influence on the spatial distribution of the materials. As the deposition of the alluvial materials is morphologically constrained by the relief, it was necessary to carefully analyze the slope and curvature of the area in order to limit the geographical extension of this primarily continuous surface (Figure 3).

3.2. Geotechnical characterization

The irregular spatial distribution of the borehole information together with the geological variability and the lateral and vertical variations in composition and geotechnical properties of the shallower layers requires a complex geotechnical model. The geotechnical characterization was performed based on the results of N_{SPT} data and lithology. A wide range of factors, which include the irregular spatial distribution and the lack of standardization in national practice, restrict the efficient use of these data. In the data analysis, despite the careful exclusion of clearly abnormal values, it has always been considered that the results are estimations that have associated uncertainties.

A total of 376 boreholes were selected for analysis in the Baixa area, which included 1398 N_{SPT} data values. Since part of the borehole information is incomplete, invalidating the application of the corrections to the SPT blow counts, it was decided to use the uncorrected value considering always the N_{SPT} value as the number of blows corresponding to 300 mm of penetration. In cases where, according to the practice adopted in Portugal, the test was suspended at 60 blows before total penetration, the value of N_{SPT} was extrapolated to 300 mm. This solution enabled the analysis of certain situations including the effect of the degradation of properties due to superficial weathering of the overconsolidated Miocene hard soils and soft rocks.

Considering the geological genesis and evolution of alluvial sedimentation and the different phases of deposition of the anthropogenic materials, it was expected that the geotechnical properties would have wide spatial variations. To check those differences, the area was divided and analyzed in 3 zones: northern, central and southern (Figure 2).

3.2.1. Anthropogenic deposits

Anthropogenic deposits, including the debris from the 1755 earthquake, have a heterogeneous lithological composition, depending on their genetic context. In most cases they are sandy. In the fluvial channel, the anthropogenic materials can be intercalated in the soft alluvial deposits making interpretation a difficult task.

The N_{SPT} values show the presence of normally consolidated soils, with 52% of the tests having values up to 10. Values higher than 50 (10%), corresponding to the presence of cobbles or larger fragments included in the softer matrix, are not representative for the behavior of these materials and were ignored (Figure 4). The statistical analysis of the N_{SPT} values shows mean values that are affected by a small number of high values. To overcome this problem, the median was used. Separate analyses are presented for tests performed at depths less than and greater than 5 m (Table 1).

The distribution of the N_{SPT} values with depth is very irregular but shows a slight trend to increasing values with increasing depths, due to the increasing over-

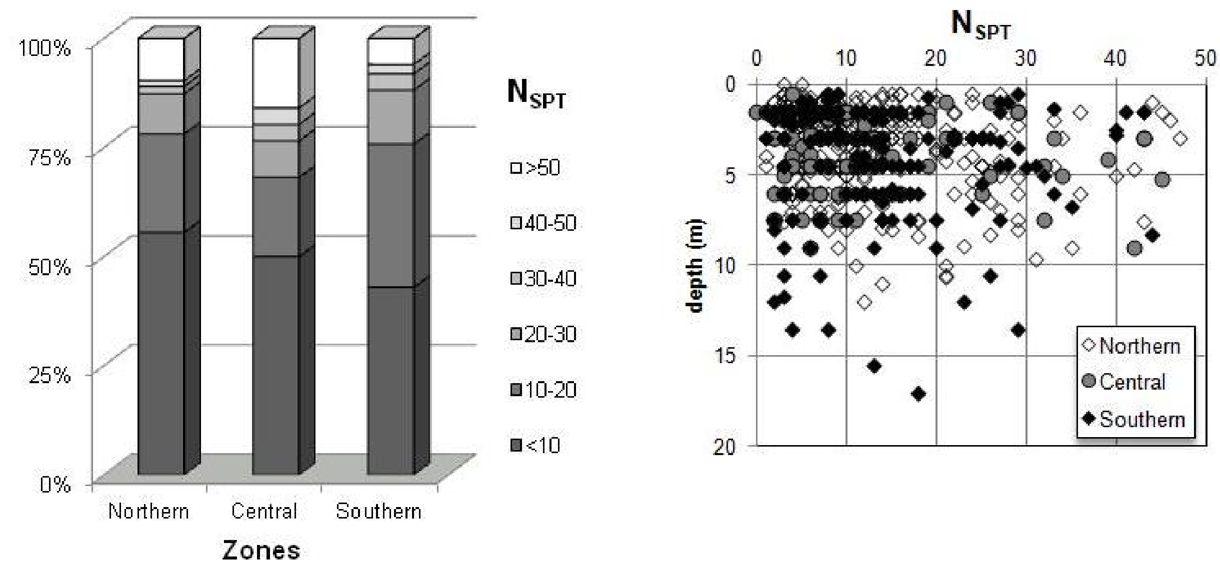

Figure 4. Distribution of N_{SPT} values in the anthropogenic deposits for the three zones. Left: histograms of N_{SPT} for depths less and greater than 5 m. Right: distribution of N_{SPT} (< 50) with depth.

Zone	Median			Total number of tests
	< 5 m	> 5 m	All tests	
Northern	8	11	9	421
Central	9	9	9	111
Southern	11	13	12	175

Table 1. Median of N_{SPT} values ($N_{SPT} < 50$) in the anthropogenic deposits at different depths for the three zones.

burden pressure (see Figure 4).

The lower values observed at greater depths in the southern zone may result from the settlement of these materials within the alluvial deposits.

In terms of the geographical distribution of the anthropogenic deposits, the analyzed values show a slight tendency towards the presence of denser materials in the upper 5 m in the central and southern zones. These results may be a consequence of the increase in densification, due to the contribution of the local dense network of short wooden piles used for foundations in the 18th-19th centuries.

3.2.2. Alluvium

The alluvial deposits are characterized by the presence of lenticular bodies and significant lateral and vertical facies variations. The main lithological facies include soft to hard silt and clay, loose to dense sands, and a range of transitional lithologies. A gravelly layer is frequently present at the bottom of the alluvial sequence.

The N_{SPT} values indicate the presence of normally and slightly overconsolidated soils (Figure 5). The lower values correspond to soft, silty and clayey soils, while the higher values correspond to sandy soils and overconsolidated intercalations resulting from the complex depositional and diagenetic history of the alluvial sequence, taking into account the effect of the water level variation and erosion episodes. Values higher than 50, probably associated with the presence of coarse particles or fragments of anthropogenic materials that have settled into the alluvial sediments, were interpreted as isolated occurrences (Figure 5). These values should not influence the overall behavior of the soils and, therefore, were ignored in the analysis. In the right-hand graphs of Figure 5, beyond the projection of the points corresponding to the tests, the lines of the values of the quartiles (Q1, Q2 and Q3) and percentiles (P10 and P90) are also shown. Given the uneven distribution of sandy and clayey layers, due to the lenticular character of the alluvial deposits, as well as the discrimination of the major lithologies, in the statistical analysis the overall results at different depths were considered (Table 2).

The very irregular distribution of the N_{SPT} values with depth can be interpreted as a result of the vertical and lateral lithological variation within the lenticular structure which also contributes to the uneven distribution of the overconsolidated layers (Figure 5).

3.2.3. Miocene bedrock

The Miocene bedrock is characterized by a sequence of sands, clays, marls, calcarenites, coquinites (a limestone conglomerate composed mainly of shell fragments) and limestones, with important vertical and lateral facies variations. The bedrock was analyzed as a single unit and not considered separately for each of the three selected zones.

The N_{SPT} values indicated the presence of overconsolidated hard soils and soft rocks, with 49% of the tests with extrapolated N_{SPT} values higher than 60 (Figure 6). The large range of values is a consequence of the heterogeneity in lithology and of the superficial degradation of the mechanical properties of the overconsolidated Miocene materials. The erosion of several hundred meters of sediments, exhumation and corresponding pedogenetic processes, have led to an increase in porosity and destruction of cementation bonds. The tests performed on the unweathered hard soils systematically produce very high resistance, with reduced sampler penetration, and very high extrapolated N_{SPT} values, while N_{SPT} values less than 30 were registered in the weathered materials, even at depths greater than 20 m (Figure 6 and Table 3). Although it is not very clear in Figure 6, due to the high number of tests and to the plotting of results of different study areas, the N_{SPT} distribution with depth shows the superficial degradation of the mechanical properties.

3.3. Estimation of physical properties (V_S and γ)

Shear wave velocity (V_S) can be obtained directly from seismic field experiments (cross-hole, down-hole, etc.). However, these methods are expensive and they are seldom performed in the urban environment. In this case, if no further data are available or detailed investigations are not possible, the very common SPT is often used. Since the 1970s, many authors have developed empirical correlations between N_{SPT} values and shear wave velocity [e.g., Imai 1977, Imai and Tonouchi 1982]. Many of the existing correlations have been derived for specific soil types and geological contexts

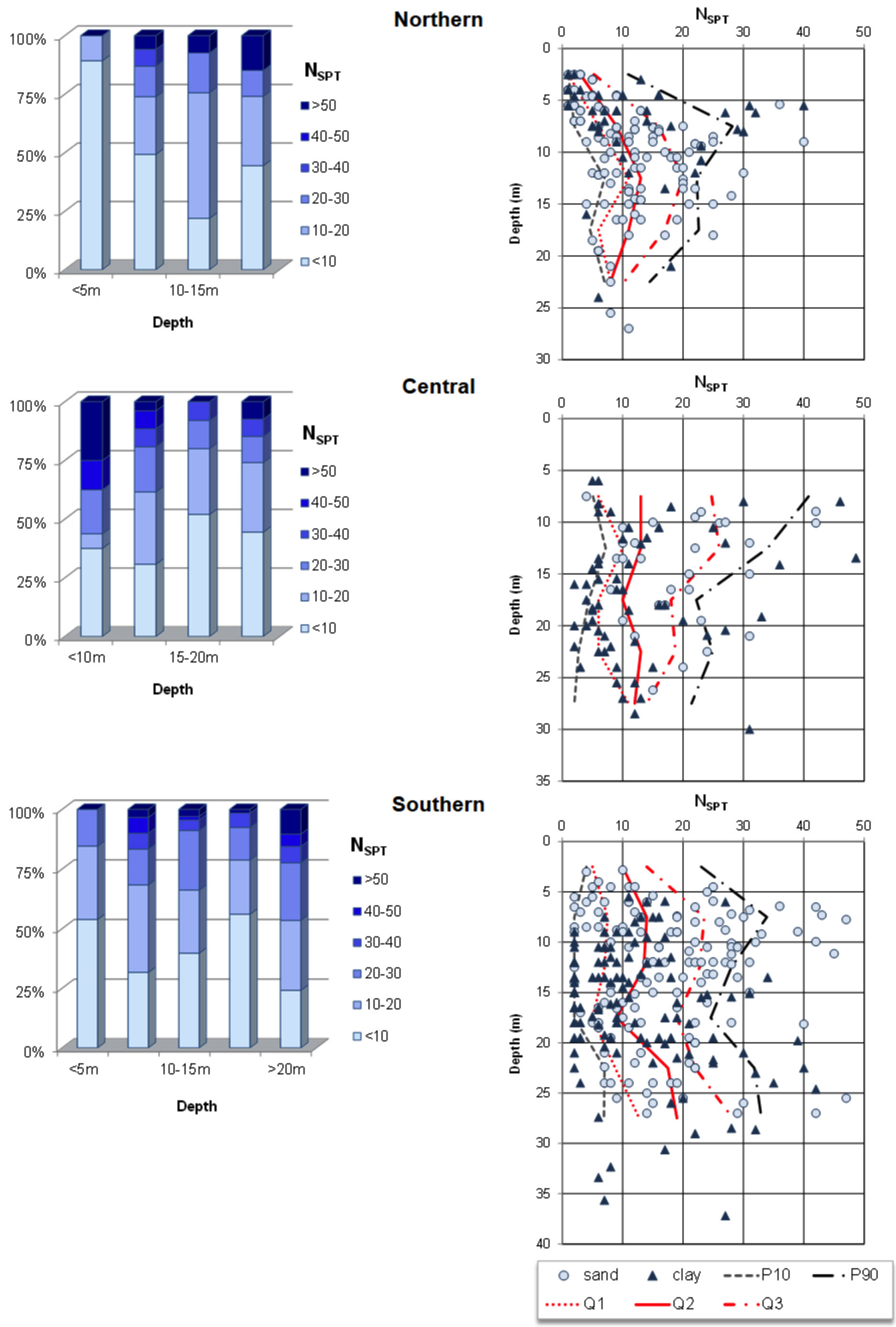

Figure 5. Distribution of N_{SPT} values in the alluvial deposits for the three zones. Left: histograms of N_{SPT} for different depths. Right: distribution of N_{SPT} (< 50) with depth for clayey and sandy materials. Percentiles lines (in black) and quartiles lines (in red) are also presented.

Zone		Median					Total number of tests
		< 5 m	5 – 10 m	10 – 15 m	15 – 20 m	> 20 m	
Northern	clay	2	9	20	7	--	44
	sand	3	9	13	11	--	110
	all	3	9	13	10	---	154
Central	clay	--	7	13	8	9	57
	sand	--	23	14	18	13	30
	all	---	13	13	10	12	87
Southern	clay	14	13	8	8	16	122
	sand	9	17	22	12	19	132
	all	10	14	14	9	18	254

Table 2. Median of N_{SPT} values (N_{SPT} < 50) in the alluvial deposits at different depths for the three zones.

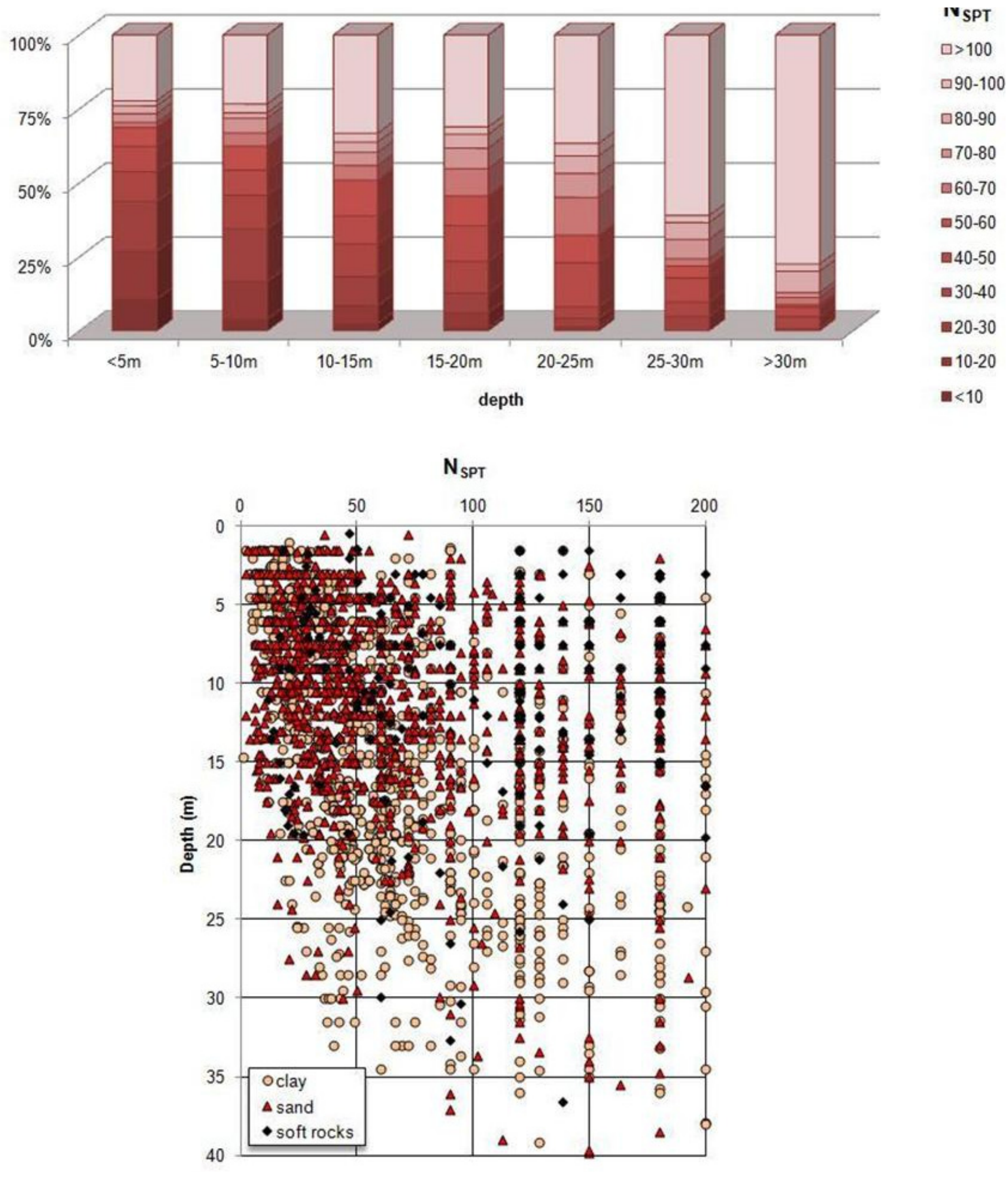

Figure 6. Distribution of N_{SPT} values in the Miocene bedrock (excluding 10% of the tests with N_{SPT} values greater than 200). Top: histograms of N_{SPT} values for different depths. Bottom: distribution of N_{SPT} values with depth.

	Quartile							Total number of tests
	< 5 m	5 − 10 m	10 − 15 m	15 − 20 m	20 − 25 m	25 − 30 m	> 30 m	
Clay	24	35	53	62	72	120	150	1384
Sand	41	50	60	64	88	100	150	1123
Soft rocks	164	150	180	180	134	105	142	308
All tests	36	44	60	64	75	120	150	2815

Table 3. Median of N_{SPT} values of the different lithologies in the Miocene formations.

while others were suggested without specific limitation. Some authors presented a set of available correlations derived by several authors to compare the range of estimated values [e.g., Jafari et al. 2002, Hasancebi and Ulusay 2007, Hanumantharao and Ramana 2008, Brandenberg et al. 2010, Maheswari et al. 2010a, Sitharam 2010, Akin et al. 2011, Nath and Thingbaijam 2011, Wair et al. 2012, Anbazhagan et al. 2012, 2013]. In the NovoSPT software (www.novotechsoftware.com/spt/) a total of 59 equations have been collected and implemented. Applying this software, Afkhami [2013] analyzed the reliability and applicability of the correlations and the importance of the geological context in the selection of the equation.

The majority of the available correlations are based on the following relationship:

$$V_S = \alpha N_{SPT}^{\beta} \quad (1)$$

The authors proposed values of α and β, for different materials (types of soils and stratigraphical context). Some examples are presented in Table 4.

Taking into consideration the lithology of each surface formation, shear wave velocities for anthropogenic deposits and for muddy and sandy alluvium were first estimated using the empirical relationships proposed by Imai [1977]. Similar expressions, derived by Lee [1990], were used to estimate the shear wave velocities of the Miocene materials (Table 4).

The N_{SPT} values associated with the different surface materials were also used to estimate the unit weight, γ (kN/m^3), according to the following expressions [Bowles 1982]:

$$\gamma = 2 \ln (N_{SPT}) + 12.1 \text{ (for alluvium)} \quad (2)$$

$$\gamma = 2.1 \ln (N_{SPT}) + 11 \text{ (for anthropogenic deposits)} \quad (3)$$

Due to the diversity of the geotechnical properties of surface materials, the range of estimated values showed large variation. Taking the median of the N_{SPT} values for the identified surface materials, V_S values ranging from 160 m/s to 188 m/s for anthropogenic deposits, 152 m/s to 187 m/s for silty and clayey alluvium, and 132 m/s to 216 m/s for sandy alluvium were obtained, with the lower values for shallower deposits and the higher values for the deeper deposits. The unit weight varied from 15.6 kN/m^3, for the most superficial anthropogenic deposits (down to 2 m), to 17.9 kN/m^3, for the deeper alluvial deposits.

For the weathered upper levels of the Miocene hard soils and soft rocks, the V_S values varied from 324 m/s to 585 m/s, according to the depth and the lithological composition. The estimated unit weight was 20 kN/m^3

α	β	Material	Author	Unit
80.6	0.331	Sand	Imai [1977]	Anthropogenic deposits
80.2	0.292	Clay	Imai [1977]	Muddy alluvium
91.0	0.337	Sand	Imai [1977]	Sandy alluvium
81.39	0.34	Undifferentiated	Rodrigues [1979]	Alluvium
51.5	0.62	Undifferentiated	Iyisan [1996]	Alluvium
27	0.73	Clay	Jafari et al. [2002]	Alluvium
58.0	0.39	Undifferentiated	Dikmen [2009]	Anthropogenic deposits
60.0	0.36	Silt	Dikmen [2009]	Muddy alluvium
73.0	0.33	Sand	Dikmen [2009]	Sandy alluvium
96.9	0.314	Stiff clay	Imai and Tonouchi [1982]	Miocene Formations
57.0	0.49	Sand	Lee [1990]	Miocene Formations

Table 4. α and β values proposed by several authors for different types of soils and stratigraphical contexts.

for weathered overconsolidated Miocene material and 22 kN/m³ for bedrock.

These values are in accordance with measured data obtained for the same types of geological formations by Almeida [1991].

4. Testing and adjusting Vs values for the shallower formations

4.1. Procedure

To constrain the shear wave velocity of the shallower formations, spectral ratios H/V computed from ambient vibration recordings were used. The H/V curves, obtained at specific sites, were compared with theoretical transfer functions computed for the soil profile, which were obtained independent of the geotechnical borehole data. The procedure consisted of five steps (Figure 7): (1) computing the H/V curve from ambient vibration records acquired at selected sites close to geotechnical boreholes; (2) identifying the 1D soil profile from the geotechnical information (thickness of each surface layer and the depth to bedrock); (3) estimating the shear wave velocity for each layer from N_{SPT} values collected from several geotechnical boreholes, using empirical relationships appropriate to the geological setting (see Table 4); (4) computing transfer functions for these soil profiles using synthetic accelerograms; (5) selecting the most appropriate empirical relationship by fitting the fundamental frequency (F_0) of the theoretical transfer functions to the peak frequency of the experimental H/V curve. This fitting took into account potential non-linear behavior of the surface deposits.

The main steps of this procedure are presented and discussed below.

4.2. H/V curves obtained from ambient vibration measurements and soil profile definition

Taking into consideration the spatial distribution of boreholes with satisfactory information, 13 sites were selected to perform ambient vibration measurements in the study area (Figure 8). The locations of the sites were chosen to sample alluvium and anthropogenic deposits with different thicknesses, and also over different Miocene formations. The measurements were carefully performed according to equipment specifications, field conditions and guidelines from the European SESAME project results [SESAME WP12 2004, Chatelain et al. 2008, Guillier et al. 2008]. Ambient vibrations were recorded for 20 to 30 minutes at each site, using a Cityshark digitizer coupled with a 3D Lennartz seismometer of 5 second period. The measurements were taken in good weather conditions (no rain and no wind), mostly during the night, and the sensor was installed, whenever possible, directly on concrete or asphalt; in some sites, the sensor was on the sidewalk.

The H/V curves were computed using Geopsy

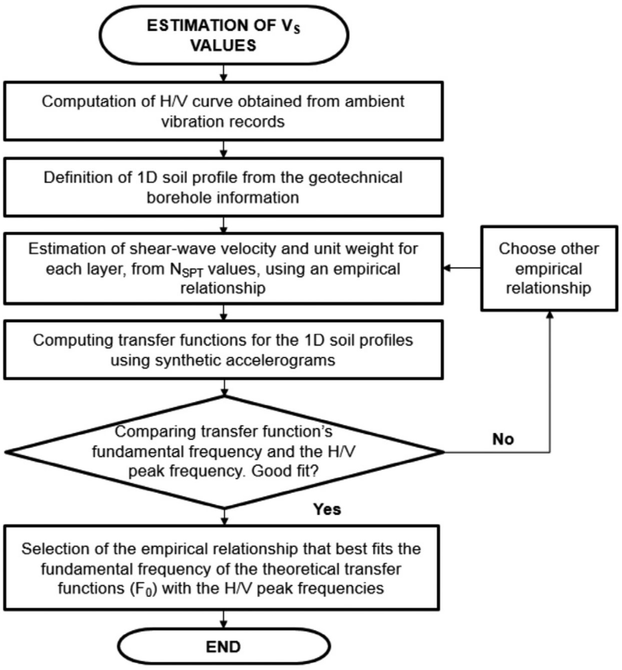

Figure 7. Synthesis of the procedure for estimating the Vs values for each layer. The empirical relationships used are presented in Table 4.

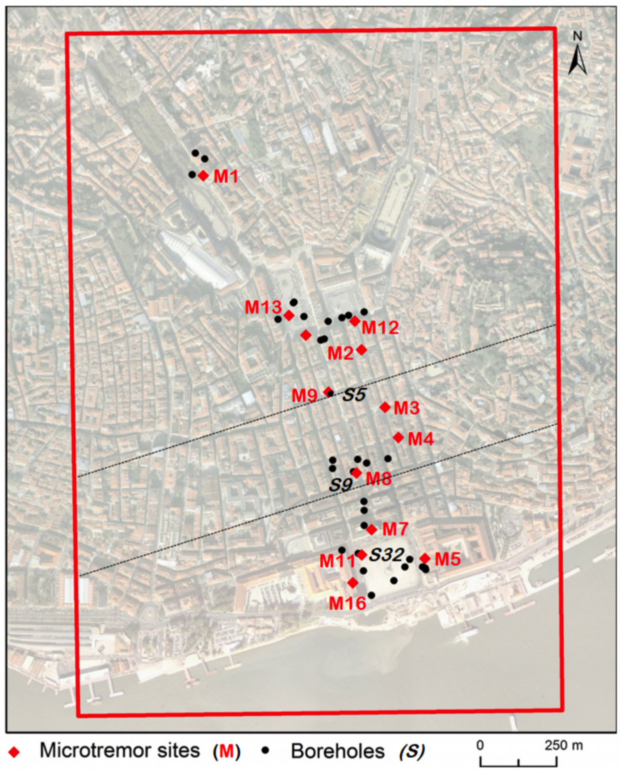

Figure 8. Location of the ambient vibration measurements (M) and the closest geotechnical boreholes (S). Boreholes used to calibrate the V_S values are identified. The dashed black lines separate the three defined zones (northern, central and southern).

software (http://www.geopsy.org/index.html), following the procedure described in detail by Chatelain et al. [2008]. In each record, stable windows with lengths between 20 s and 40 s duration were selected using an anti-triggering system [SESAME WP12 2004, Chatelain et al. 2008]. Only records with at least 20 windows were processed. Fourier spectra were computed for each window of each component (V = vertical component; NS and EW = horizontal components). After smoothing and merging the horizontal components with a quadratic mean, the H/V curve was computed for each window. Besides all individual H/V curves, the results present the averaged H/V curve and its standard deviation computed on a decimal logarithmic scale. Standard deviation for F_0 (H/V peak frequency) was also computed from the F_0 values obtained for each individual window. The H/V curves are displayed in Figure 9 and the corresponding F_0 and A_0 values are presented in Table 5.

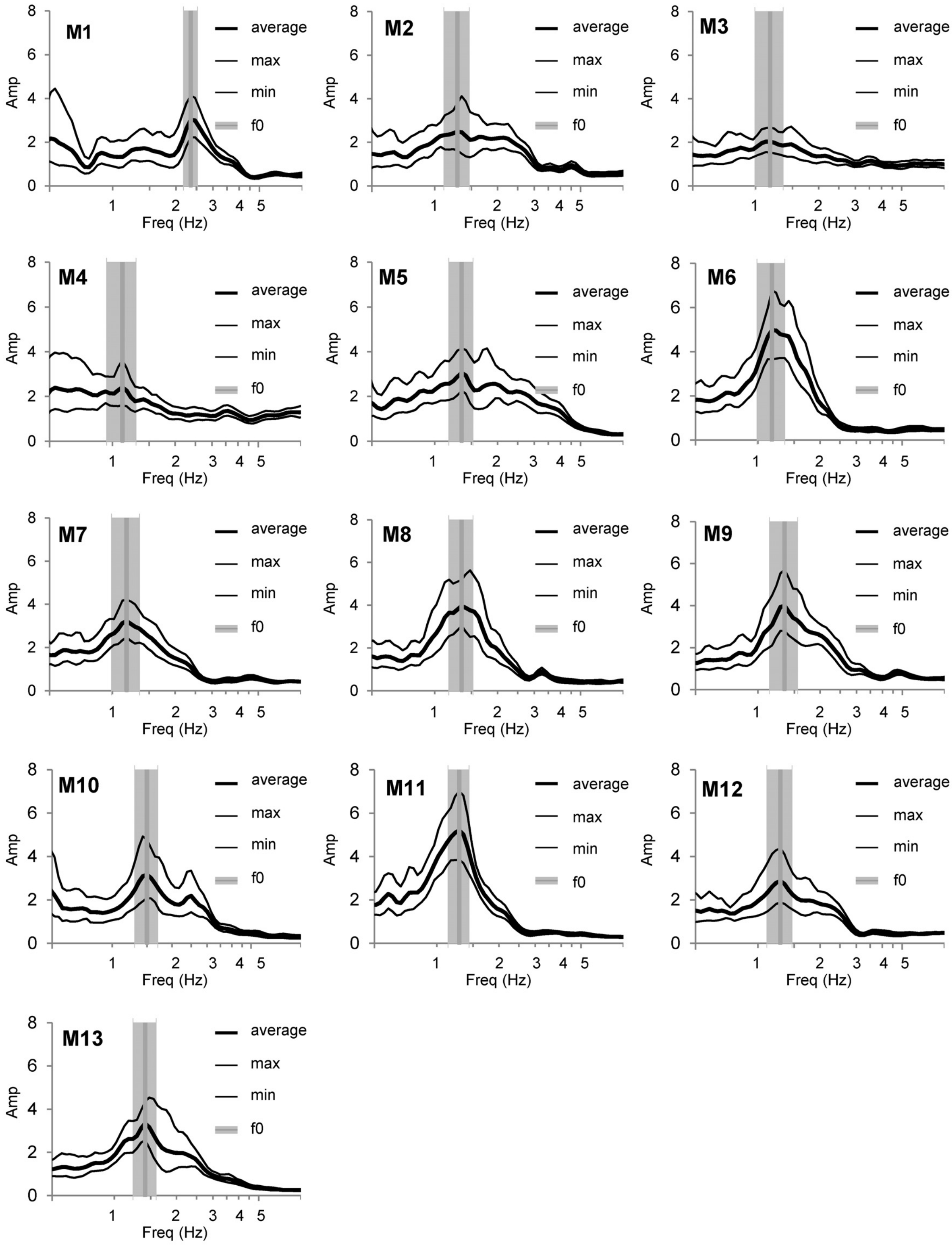

Figure 9. H/V curves computed for each site.

Site	F_0	σ (F_0)	A_0	σ (A_0)
M1	2.4	0.20	3.0	1.36
M2	1.3	0.27	2.5	1.53
M3	1.2	0.23	2.0	1.32
M4	1.1	0.19	2.4	1.50
M5	1.3	0.25	3.1	1.36
M6	1.2	0.12	5.0	1.36
M7	1.2	0.17	3.2	1.31
M8	1.3	0.18	4.0	1.31
M9	1.3	0.21	4.0	1.43
M10	1.3	0.22	3.2	1.51
M11	1.3	0.15	5.2	1.35
M12	1.3	0.20	2.9	1.53
M13	1.4	0.23	3.3	1.31

Table 5. Peak frequency (F_0) and corresponding amplitude (A_0) of the H/V curve obtained at each site. Corresponding standard deviations are also presented.

All computed H/V curves satisfy the reliability criteria defined in Sesame guidelines [SESAME WP12 2004], but 5 of these curves did not satisfy the clear peak criteria (sites M3, M4, M6, M7 and M8). Sites M3 and M4 are located on the Colina do Castelo foothills, over a Miocene bedrock formation with no soft surface deposit; so, it is not surprising that the H/V peaks are not very pronounced. The failure of the clear peak criteria for sites M6 and M8 is due to the existence of two very close peaks (see Figure 9). For site M7 the failure of these criteria is due to the "high" values of the H/V curve presented at lower frequencies (compared with the peak amplitude). However, it was noticed by Haghshenas et al. [2008] that the clear peak criteria recommended in the SESAME guidelines are too strict. This is particularly true when the fundamental frequency is low, as many criteria allow a variation within a small percentage of F_0 (for instance 5 to 10%). As F_0 in Baixa varies between 1.1 and 1.4 (see Table 5), the acceptable interval is very small and so it was decided to consider all H/V curves in the following discussion.

From the analysis of the H/V curves displayed in Figure 9 and the values presented in Table 5, it is possible to observe that the average fundamental frequency of Baixa lies between 1.2 Hz and 1.4 Hz. Only the most northern site (M1), already outside the main area of Baixa, has a fundamental frequency of 2.4 Hz. With the exception of the sites over the Miocene bedrock formations (M2, M3 and M4), the amplitude of these frequency peaks varies from 2.9 to 5.2. As expected, the sites over the Miocene bedrock formations show a very poorly-defined peak.

To compute the transfer functions and perform V_S estimation (next step), three soil profiles (one for each zone) were defined from three geotechnical boreholes selected close to sites where ambient vibration measurements were performed (Figure 8): M9 (for the northern part; borehole S5), M8 (for the central part; borehole S9) and M11 (for the southern part; borehole S32).

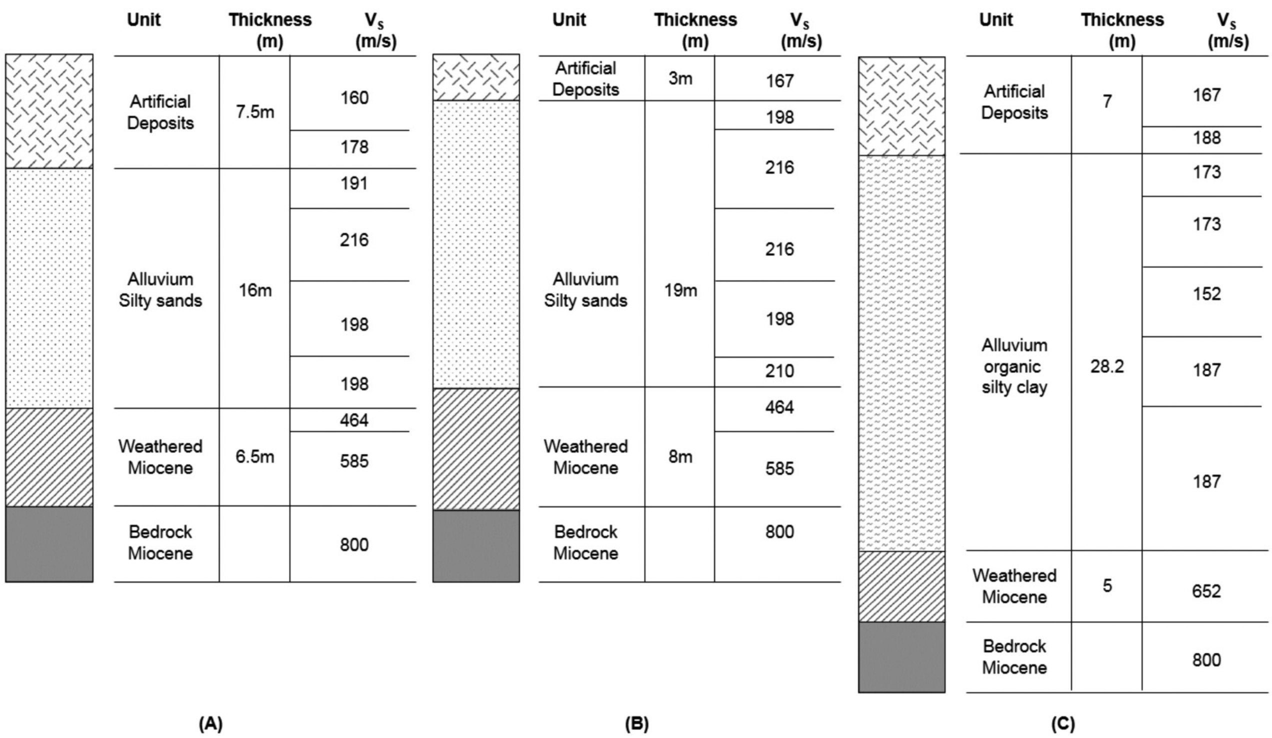

Figure 10. Soil profiles used to calibrate the V_S values: (A) S5; (B) S9; (C) (S32)

From the borehole information the lithology and thickness of each layer, as well as depth to bedrock, were defined. The shear wave velocity and unit weight were computed applying the empirical expressions presented above to the respective N_{SPT} (median values) for each layer. For bedrock (composed of unweathered Miocene rocks), shear wave velocity was set at 800 m/s and the unit weight equal to 22 kN/m^3. Figure 10 presents the three test soil profiles.

4.3. Computing transfer functions and estimating V_S

Transfer functions can be defined as the ratio between the Fourier amplitude spectra of the seismic motion at the surface and the seismic motion at at the bedrock surface [Kramer 1996]. To define the bedrock input motion Lisbon's historical seismicity, as well as the seismic code for mainland Portugal [Costa et al. 2008], have been taken into account. Two different types of input motion corresponding to relevant scenarios were selected: (i) a distant earthquake (d = 200 km) with large magnitude (M = 7.9) and (ii) a nearby earthquake (d = 25 km) with smaller magnitude (M = 6.0). These two scenarios, similar to the ones proposed by other authors [Carvalho et al. 2008, Oliveira 2008], can be associated with several past earthquakes that affected Lisbon, for instance, the nearby January 26, 1531, (M = 7) and April 23, 1909, (Mw = 6.1) earthquakes, from Lower Tagus Valley sources, and the distant larger magnitude earthquakes of November 1st, 1755 (M = 8.5), and February 28, 1969 (M = 7.9), from offshore sources. Due to the non-existence of strong motion records on the Portugal mainland, within these magnitude and distance ranges [Vilanova et al. 2009], synthetic accelerograms were computed to simulate the strong motion associated with each scenario.

The synthetic accelerograms, generated through a physical simulation of the fault rupture and travel path mechanisms using stochastic methods [Estêvão and Oliveira 2012], were computed specifically for this study. With this method, it was possible to select the inland and offshore sources associated with the close and distant earthquake scenarios. The corresponding seismic motions are in accordance with the two types of seismic action defined in EC8 for mainland Portugal [Costa et al. 2008]. For each source ten synthetic accelerograms were computed. Figure 11 presents the response spectra of each seismic motion, for the two scenarios, as well as the Portuguese seismic code response spectra for a 475 year return period [IPQ 2010]. Mean PGA are 1.58 m/s^2 (0.16 g) for the near-field and 1.22 m/s^2 (0.12 g) for the far-field simulated seismic motions. These values are smaller than the ones specified in the Portuguese code [IPQ 2010]; however they are in agreement with the attenuation law derived by Ambraseys et al. [1996] using real European strong motion records.

Several methods could be used to compute the 1D soil response. Most authors agree that soft soils subjected to strong ground motions present non-linear behavior [Hartzell et al. 2004]. Simple approaches are commonly used, such as the equivalent linear method, which approximates the soil behavior using an iterative procedure [Schnabel et al. 1972], and the frequency dependent linear methods, which were proposed to improve the accuracy of the approximate solution and better simulate a wide range of shear strains [Yoshida et al. 2002]. However, as shown by Kwak et al. [2008] these latter methods may lead to different results depending on the frequency dependent algorithms used and do not always improve the accuracy of the solution.

It is also recognized that the 1D equivalent linear analysis provides a reasonable estimate of ground vibration under a seismic event [Idriss 1990]. In general, this approach is conservative compared with the results obtained by other methods using recorded or artificial accelerograms [Castellaro and Mulargia 2014]. Being aware of the analytical limitations and considering that there was insufficient information about the behavior of Baixa soils, it was decided to use the equivalent linear

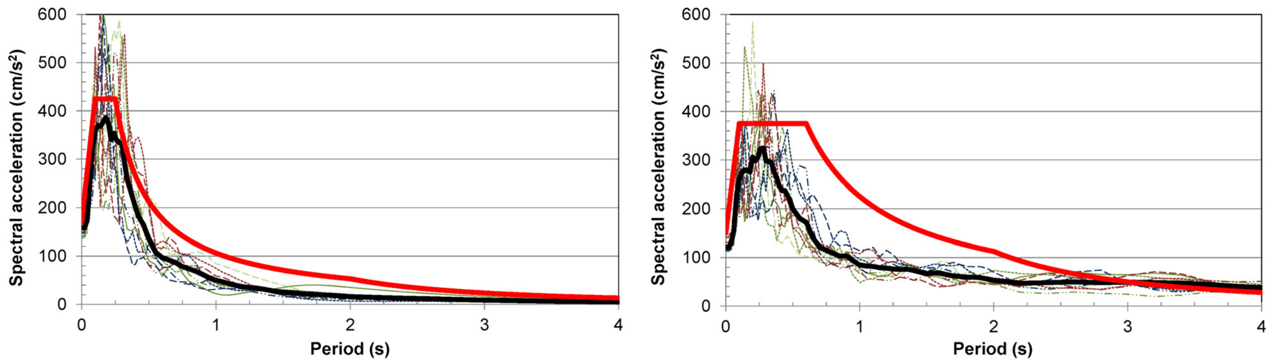

Figure 11. Response spectra for the 10 seismic motions computed for each source: (left) near-field seismic motion; (right) far-field seismic motion. The mean of the 10 spectra are presented in bold (black curve). Bold red curve: Portuguese seismic code response spectra for 475 year return period.

model to compute the 1D site response analysis, as it is implemented in the ProShake (n.d.) software [Schnabel et al. 1972]. To take into account the soil behavior, modulus ratio and damping ratio curves were selected from the literature according to the lithology present in the different layers [Seed and Idriss 1970, Sun et al. 1988].

The computed transfer functions for each soil profile were compared with the corresponding H/V curves obtained from the ambient vibration analysis at the same site, to check for the similarity between the fundamental frequencies of the transfer functions (F_0) and the H/V frequency peaks. In spite of the large difference in the strains involved on ambient vibrations and simulated seismic input motions, several authors agree that the peak frequency derived from the H/V curves provides a very satisfactory estimate of the natural frequency of the soil deposit [Bard 1999]. Haghshenas et al. [2008] compared the fundamental frequency obtained from spectral ratios to a reference site using earthquake records and the H/V frequency peak obtained with ambient vibrations. They examined several sites with different site conditions, and they found a generally good agreement between the fundamental frequencies obtained with both techniques for most of the analyzed sites. However, since strong seismic motions and soft soils are involved, the occurrence of non-linear effects must be considered.

To illustrate the procedure, Figure 12 displays the comparison between one theoretical transfer function, for each simulated seismic motion, and the H/V

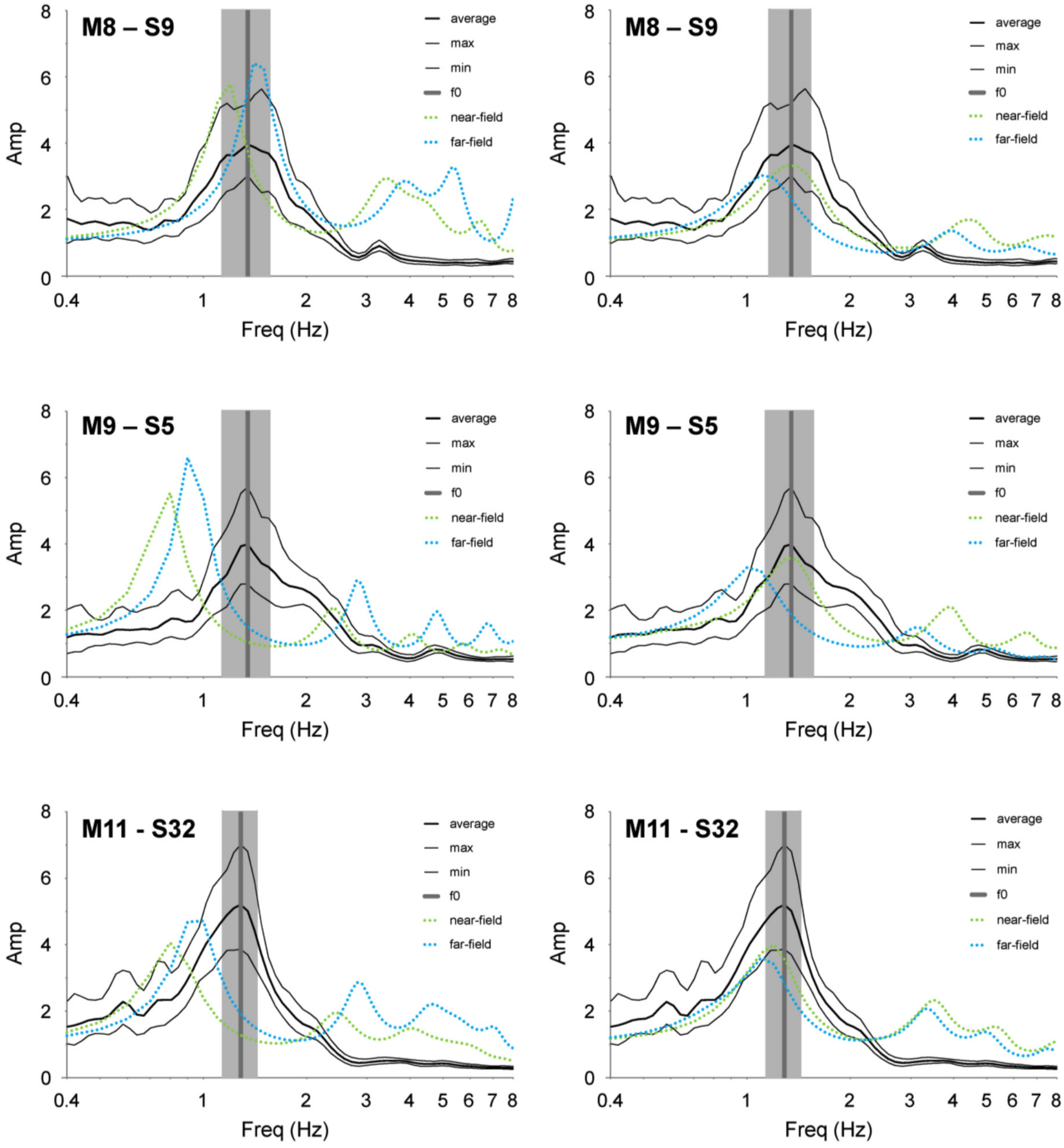

Figure 12. Comparison between the computed transfer functions and the H/V curves obtained from ambient vibration analysis. Left: transfer functions computed with the first estimated V_S values. Right: transfer functions computed with the final estimated V_S values.

curves. It can be seen that F_0 did not fit the H/V peaks as expected (plots on the left-hand side). Considering that the main parameters affecting the soil response are the thickness and the shear-wave velocity of each layer, it is necessary to change one of these two parameters to have a better compatibility between the transfer function and the H/V curve peaks. As the geometry of the soil profile cannot be changed (it is constrained by the geotechnical borehole information), the disagreement is likely to be due to a wrong estimation of the V_S values. So, the V_S values were adjusted, using different empirical relationships [e.g., Rodrigues 1979, Imai and Tonouchi 1982, Iyisan 1996, Jafari et al. 2002]. Also, taking into consideration that the non-linear behavior can decrease the amplitude of the frequency peak and shift it to lower frequencies [Régnier et al. 2013], final relationships that provided transfer functions with fundamental frequency closer to the H/V frequency peaks were selected. The comparison between the final transfer functions and the H/V curves is displayed on the right-hand side of Figure 12; the empirical relationships selected were derived by Dikmen [2009] (see Table 4). Final V_S values vary from 131 m/s to 158 m/s for anthropogenic deposits, from 132 m/s to 170 m/s for silty and clayey alluvium (Baixa southern zone), and from 105 m/s to 170 m/s for sandy alluvium (Baixa northern and central zones). The unit weight was set equal to 16 kN/m^3 for anthropogenic deposits and to 18 kN/m^3 for alluvial deposits, which are in the range of measured values for the same types of materials [Almeida 1991]. For the overconsolidated Miocene material, V_S velocities of 400 m/s for sand and sandstone, and 450 m/s for clay and limestone, were assumed; the unit weight was kept equal to 20 kN/m^3. The bedrock properties were not changed. Table 6 presents the initial and final V_S values.

These values should be checked against experimental measurements. In the Baixa area, only one direct measurement was performed (cross-hole test) giving values that are slightly higher, between 150 m/s and 240 m/s [LNEC 1998]. Geotechnical studies for site characterization before the construction of the Vasco da Gama Bridge, which crosses the Tagus estuary north of Lisbon, were performed in the Tagus alluvium about 9 km from Baixa [Oliveira et al. 1997]. This alluvium was divided into 6 sub-units, 4 of them with composition and geotechnical properties similar to the Baixa alluvium. Seismic cross-hole experiments gave shear wave velocities for these 4 sub-units varying from 51 m/s to 348 m/s. The usual range of V_S values for the

Initial and Final V_S values obtained from N_{SPT}	Anthropogenic deposits	Depth	< 5 m	> 5 m		Reference
		N_{SPT}	8 - 11	9 - 13		
		V_S (initial)	160 - 178	167 - 188		Imai [1977]
		V_S (final)	131 - 148	137 - 158		Dikmen [2009]
	Alluvium		Northern zone	Central zone	Southern zone	Reference
		N_{SPT}	3 - 13	10 - 13	9 - 18	
		V_S (initial)	132 - 216	198 - 216	152 - 187	Imai [1977]
		V_S (final)	105 - 170	156 - 170	132 - 170	Dikmen [2009]
	Miocene	Depth	0 - 10 m	10 - 30 m	> 30 m	Reference
		N_{SPT}	36 - 44	60 - 120	150	
		V_S (initial)	330 364	424 - 595	664	Lee [1990]
		V_S (final)	400 - 450	400 - 450	800 (*)	
V_S values obtained from field experiments	Alluvium	Vs range	Experiment	Local	Distance	Reference
		150 - 240	Cross-hole	Baixa	----	LNEC [1998]
		140 - 290	Cross-hole	Alcântara, Lisbon	3.4 km	Freitas et al. [2014]
		51 - 348	Cross-hole	Sacavém	9 km	Oliveira et al. [1997]
		100 - 230	SASW	Sta Iria da Azóia - Forte da Casa	15 - 19 km	Lopes [2005]
		110 (**)	SASW	Póvoa de Santa Iria	18 km	Lopes et al. [2005]

Table 6. Initial and final V_S values obtained from N_{SPT} relationships (three first rows) and V_S values obtained from field experiments (last row). All V_S values are in m/s. (*) At depths greater than 30 m, the Miocene formations were considered as bedrock. (**) Single experiment performed for a 7 m thick alluvium layer

Tagus estuary alluvium lies between 100 m/s and 230 m/s, often with higher values for the deeper layers [Lopes 2005]. Freitas et al. [2014] obtained values from 140 m/s to 290 m/s from cross-hole experiments performed in Tagus alluvium at a site in the Alcântara Valley, located approximately 3.4 km west of Baixa. Lopes et al. [2005] obtained a value of 110 m/s for the shear wave velocity of an alluvial deposit 7 m thick, also close to the Tagus River, a little further north of Lisbon, from spectral analysis of surface waves (SASW). These experimental values are also summarized in Table 6.

Considering the wide range of measured and calculated values from in situ experiments, the values estimated for downtown Lisbon, using the mentioned empirical relationship, seem realistic.

5. Spectral response of downtown Lisbon

To produce a map of the spectral response of the Baixa area, a set of 13 cross-sections parallel to the river bank and regularly spaced at 100 m intervals was produced. For each cross-section, a set of soil profiles spaced at 50 m intervals were defined, using data retrieved from the subsurface model. A total of 256 soil profiles were uniquely identified (Figure 13A). The depth and thickness of the anthropogenic deposits and of the alluvial deposits were defined using the geological 3D model, as well as the identification of the bedrock geological formation (Figure 13B).

Two sets of 10 transfer functions, corresponding to the near-field seismic motions and to the far-field seismic motions, were computed for each soil profile. For each soil profile the transfer functions for the two types of seismic motion were not very different (see Figure 13C,D). So, it was decided to consider the mean transfer function, for each soil profile and for each type of seismic motion (near-field and far-field), to present and discuss the results.

Figure 14 shows the obtained fundamental frequencies, as well as the corresponding amplification factors, for each type of seismic motion. For both scenarios it can be seen that the fundamental frequency of the Baixa area lies between 1.2 Hz and 2 Hz in the middle of valley, reaching 3 Hz near the edges where the anthropogenic and alluvial deposits have less expression. Higher frequencies, up to 10 Hz, are observed outside the valley over the Miocene formations. This result is in accordance with the predominant frequencies of the first microzonation map obtained by ambient vibration analysis for the Lisbon town by Teves-Costa et al. [1995]. The amplification factors for these funda-

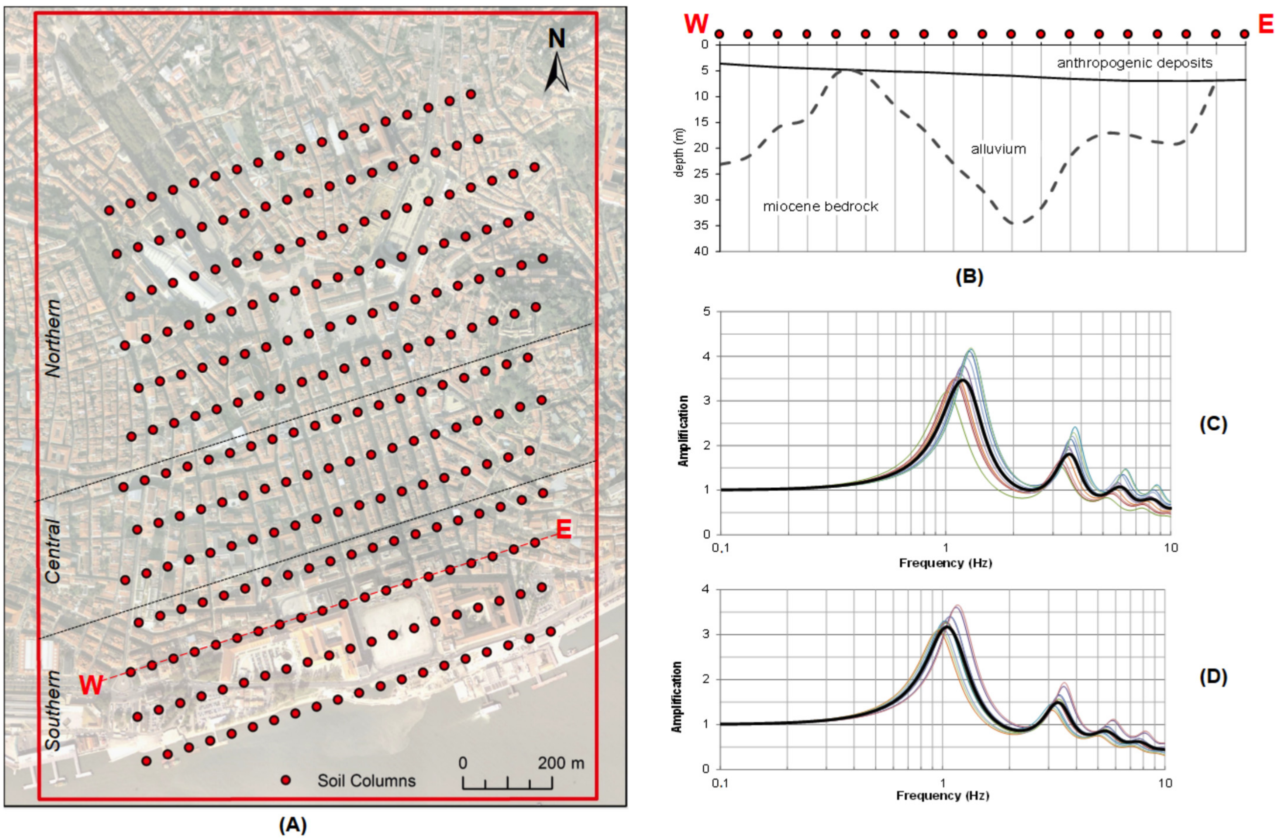

Figure 13. Location of the 256 soil profiles for which the transfer functions were computed (A). Example of one cross section performed to define the soil profiles (B). Transfer functions computed for 10 near-field (C) and 10 far-field (D) seismic motions for an arbitrary profile. The black bold curves are the mean transfer functions for each type of motion.

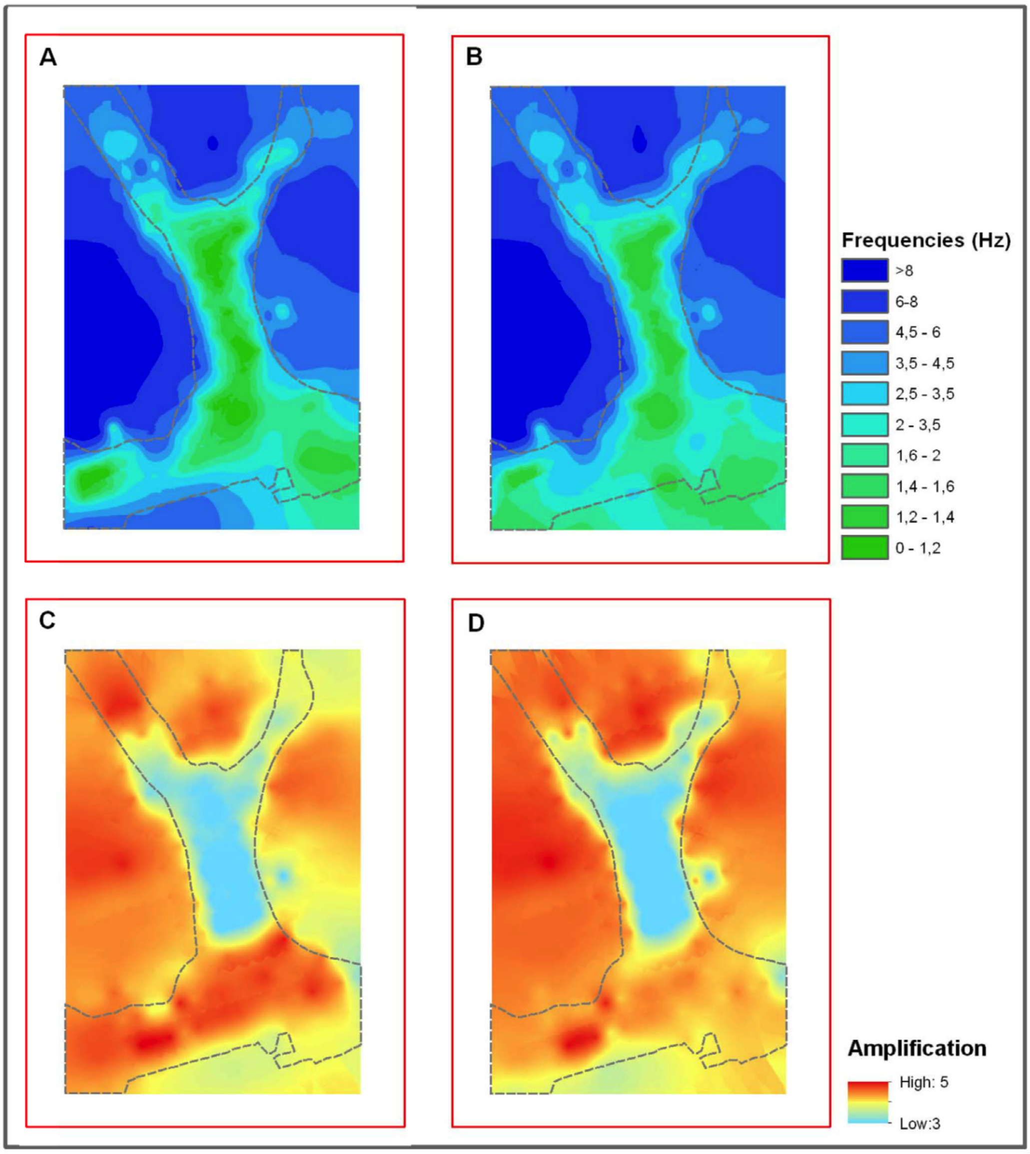

Figure 14. Fundamental frequencies (top) and the corresponding amplifications (bottom) for a near-field seismic motion (left) and a far-field seismic motion (right).

mental frequencies vary from 3.8 to 4.4 in the northern and central zones of the valley, reaching 5 in the southern zone. Differences between the near-field motion and the far-field motion simulations are not very sharp.

It was expected that some correlation between the alluvium thickness and the fundamental frequency of the soil would be observed. However this is not very pronounced. In detail, it is possible to observe that the fundamental frequencies for the near-field motion seem to better represent the thickness of the alluvium deposits (Figure 14A); however, the variability of the thickness of the anthropogenic deposits can mask the expected effect. Comparing Figure 14C and D it is possible to observe that the amplification is a little lower in the middle of the valley for the far-field seismic motion and a little higher in the southern zone for the near-field motion. However, as mentioned, these differences are very small (less than or equal to 0.4). As a whole, this is a very consistent result.

The spectral responses at 1 Hz and 2.5 Hz are displayed in Figure 15. It is clear that these responses are very similar for both seismic motions. The spectral amplitude at 1 Hz (Figure 15A,B) reaches a maximum of 4 in the middle of the valley, and it seems to correlate well with the thickness of the alluvial deposits. The spectral amplitude at 2.5 Hz (Figure 15C,D) is close to 1 in the central zone of the valley, reaching 3.5 in the northern zone, and it exceeds 5 in some areas in the southern zone of the valley. This effect could be associated with a local increase in the thickness of the superficial deposits, in the southeastern areas, whereas in the southwestern zone this effect is related to the response at a single point that has an abnormal thickness of anthropogenic deposits and it should be further investigated.

The analysis of the spectral amplitude at 2.5 Hz, which is similar both for near- and far-field seismic mo-

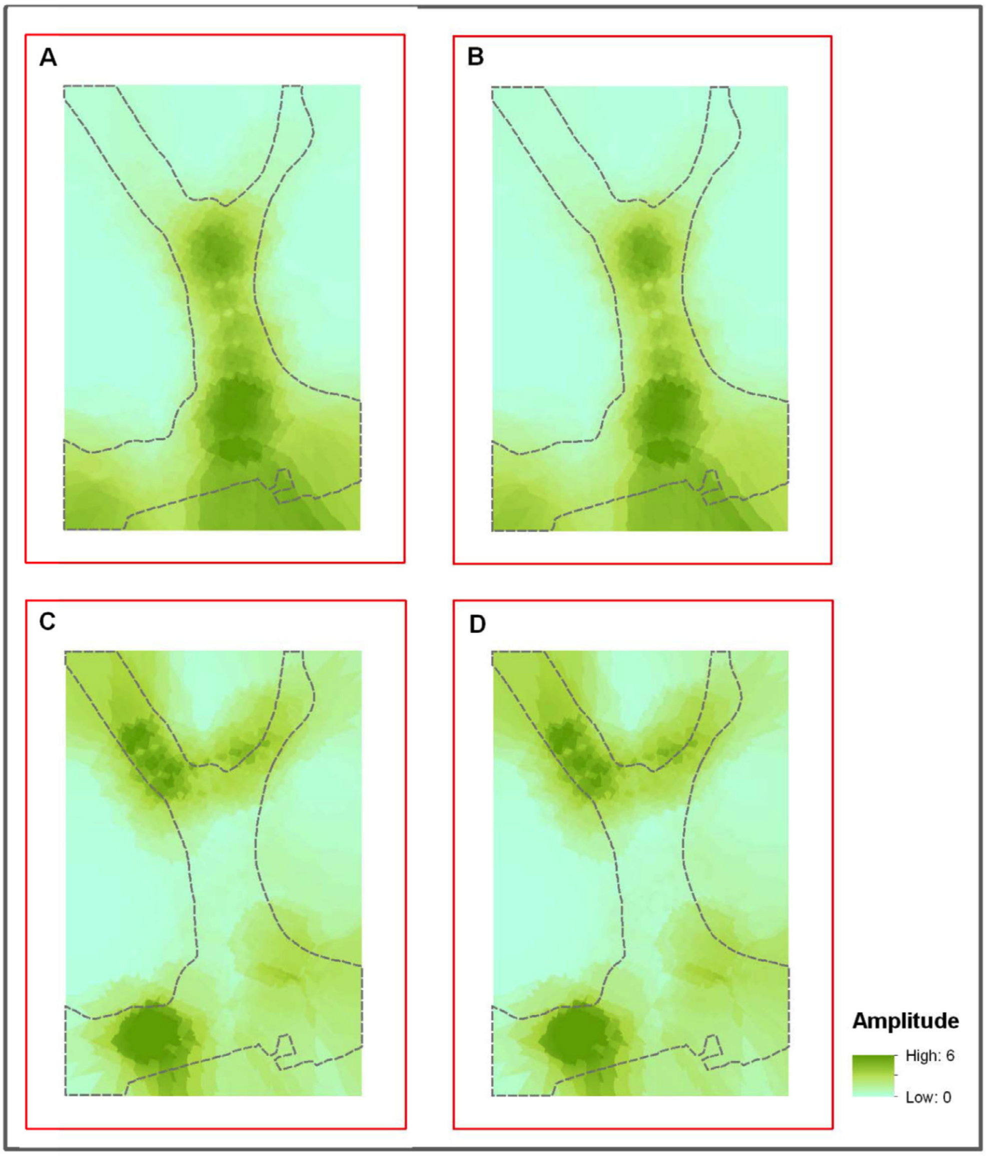

Figure 15. Spectral amplitude at 1 Hz (top) and 2.5 Hz (bottom) for a near-field seismic motion (left) and a far-field seismic motion (right).

tions, is very important because this frequency is within the range of the natural frequency of the Baixa building stock which varies from 2.3 Hz to 3 Hz [Oliveira 2004].

6. Conclusions

In this paper, the use of the Lisbon geological and geotechnical database, developed in the project GeoSIS_Lx (http://geosislx.cm-lisboa.pt), for site characterization and microzonation purposes has been tested. The identification of some inconsistencies and some shortcomings in data organization were identified during data processing (only using the database with different objectives enables the identification of its weaknesses). On the one hand, this limited the accuracy of the results and identified the need to use more efficient approaches for data processing. However, on the other hand, this contributes to the improvement of the database that has been continuously updated. As expected, the results show spatial variability conditioned by the irregular geographical distribution of the data.

Aware of these limitations, the geotechnical characterization and the definition of 1D soil profiles were performed making use of the information included in the database. Shear-wave velocities for the different layers were estimated using empirical correlations between N_{SPT} and V_S from the literature. The selection of the most suitable correlation was performed with the help of ambient vibration analysis (H/V curves). Dikmen [2009] relationships were found to be the most suitable for Baixa surface materials and the final V_S values are in the range of those obtained during experimental tests performed at different sites in the Tagus estuary for the same types of materials. All these values should be checked with experimental measurements or complementary techniques performed *in situ*. In spite of the constraints, this methodology allowed the estimation of the physical properties of the shallower formations, and it seems to be applicable in regions where no geophysical data exist but geotechnical data are commonly available.

Simple 1D equivalent linear analysis was undertaken, despite the possible existence of non-linear and/or 2D effects. The lack of knowledge about the non-linear dynamic parameters of Baixa's soils made the choice of this simple approach necessary. The numerical simulations were performed using synthetic accelerograms due to the fact that there are no real strong motion records in the Lisbon area. The results show that the fundamental frequency of Lisbon downtown shallow formations lies between 1.2 Hz and 2 Hz, reaching 3 Hz at the edges of the valley, with amplification factors of 3.8 to 4 in the northern and central zones of the valley and reaching 5 in the southern zone. These results are in agreement with the natural frequencies derived from ambient vibration records [Teves-Costa et al. 1995] and with the microzonation study of Lisbon performed by Teves-Costa et al. [2001] using numerical simulations: natural frequency for the Baixa area was about 2 Hz (or less) and the amplification factors can reach 5. However, these previous studies were done for the whole of Lisbon and only two to four simulated/sampled points were in Baixa itself. The detail of this study was much higher, enabling identification of differences in the Baixa area.

Spectral responses at 1 Hz and 2.5 Hz are similar for both near-field and far-field seismic motions. This can be conditioned by the seismic input motions used in the computations. The use of real accelerograms and the introduction of non-linear models could change the results and improve the simulations. However, the main goal of the paper was to show the applicability of the geological and geotechnical Lisbon database on microzonation studies and, for this, it was not imperative to compute an accurate response for the Baixa's shallower formations.

Taking into consideration that most of the local building stock has natural frequencies between 2.3 Hz and 3 Hz, and although a simple approach was used, resonant effects during a future earthquake that could produce an increase in the estimated level of damage can be expected. Whatever the seismic source considered, it is possible to predict that the natural frequency of Lisbon downtown (Baixa) will play an important role during the next earthquake in Lisbon.

Acknowledgements. The authors would like to thanks João Estêvão for computing the synthetic accelerograms, Martin Culshaw for his critical review, Liz and Pedro Tavares for their carefully English revision, and the two anonymous reviewers and the associated editor for their pertinent comments and suggestions. Figure 1 was produced using Google Inc. (2013), Google Earth (version 7.1.2.2041). This research was partially supported by projects GeoSIS_Lx (PTDC/ECM/64167/2006) and FCT-PEST-OE/CTE/LA00 19/2013-2014, funded by the Portuguese Foundation for Science and Technology (FCT), and Avaliação de Riscos na Cidade de Lisboa Project (LISBOA-02-3207-FEDER-000044), funded by the Comissão de Coordenação e Desenvolvimento Regional de Lisboa e Vale do Tejo under the Program QREN_PORL and by the Fundação da Faculdade de Ciências da Universidade de Lisboa (FFCUL).

References

Afkhami, A. (2013). Reliability and applicability of SPT correlations with shear wave velocity, Novo Tech Software Ltd (www.NovotechSoftware.com).

Akbari, M., M. Ghafoori, N.H. Moghaddas and G.R. Lashkaripour (2011). Seismic microzonation of Mashhad city, northeast Iran, Annals of Geophysics, 54 (4), 424-434.

Akin, M.K., S.L. Kramer and T. Topal (2011). Empirical correlations of shear wave velocity (Vs) and penetration resistance (SPT-N) for different soils in an earthquake-prone area (Erbaa-Turkey), Eng. Geol., 119, 1-17.

Almeida, F.M. (1986). Geological Map of Lisbon Council 1:10,000, Serviços Geológicos de Portugal, Lisbon (in Portuguese).

Almeida, I.M. (1991). Geotechnical characterization of Lisbon soils, PhD Thesis, University of Lisbon, 485 pp. (in Portuguese).

Almeida, I.M., G. Almeida, C. Pinto, G. Espírito-Santo and J. Vicente (2008). Geotechnical subsoil modeling using GIS with geotechnical and archaeological databases, Proc. II Europ. Conf. Int. Ass. Eng. Geol. (Madrid, September 15-19), CD-ROM, 8 pp.

Almeida, I.M., C.F. Andrade, M.C. Freitas, J. Moreno, M.C. Cabral, S. Calado and F.M.F. Marques (2009). Holocene paleoenvironmental evolution of the Lisbon downtown area as recorded in the Esteiro da Baixa sediments - first results, Proc. ICS2009, J. Coastal Res., SI 56, 574-578.

Almeida, I.M., R. Matildes, R. Taborda, D. Carreira, C. Pinto and F.T. Jeremias (2010). GeoSIS_Lx a geoscientific information system for Lisbon geotechnical data management, Proc. 11th IAEG Congress - Geologically Active, New Zealand, Taylor Williams & Francis Group, London, 1611-1618.

Ambraseys, N.N., K.A. Simpson and J.J. Bommer (1996). Prediction of horizontal response spectra in Europe, Earthq. Eng. Struct. Dyn., 25 (4), 371-400.

Anbazhagan, P., and T.G. Sitharam (2008). Seismic microzonation of Bangalore, India, J. Earth Syst. Sci., 117 (S2), 833-852.

Anbazhagan, P., A. Parihar and H.N. Rashmi (2012). Review of correlations between SPT N and shear modulus: A new correlation applicable to any region, Soil Dyn. Earthq. Eng., 36, 52-69.

Anbazhagan, P., A. Kumar and T.G. Sitharam (2013). Seismic site classification and correlation between Standard Penetration Test N value and shear wave velocity for Lucknow City in Indo-Gangetic basin, Pure Appl. Geophys., 170, 299-318

Ansal, A., M. Erdik, J. Studer, S. Springman, J. Laue, J. Buchheister, D. Giardini, D. Fäh and D. Koksal (2004). Seismic microzonation for earthquake risk mitigation in Turkey, Proc. 13th World Conf. Earthq. Eng., Vancouver, BC, paper 1428.

Ansal, A., G. Tönük and A. Kurtulus (2010). Microzonation for earthquake scenarios, In: M. Garevski and A. Ansal (eds.), Earthquake engineering in Europe, Springer, 45-65.

Bakir, S., H. Sukuoglu and T. Yilmaz (2002). An overview of local site effects and the associated building damage in Adapazari during the 17 August 1999 Izmit earthquake, B. Seismol. Soc. Am., 92 (1), 509-526.

Bard, P.-Y., and M. Bouchon (1985). The two-dimensional resonance of sediment-filled valleys, B. Seismol. Soc. Am., 75, 519-541.

Bard, P.-Y., A.-M. Duval, B. Lebrun, C. Lachet, J. Riepl and D. Hatzfeld (1997). Reliability of the H/V technique for site effect measurement: an experimental assessment, Proc.17th Int. Conf. Soil Dyn. Earthq. Eng., Istanbul, (Invited Conference).

Bard, P.-Y. (1999). Microtremor measurements: a tool for site effect estimation?, In: K. Irikura, K. Kudo, H. Okada and T. Satasani (eds.), The effects of surface geology on seismic motion, Balkema, Rotterdam, 1251-1279.

Bonnefoy-Claudet, S., P.-Y. Bard and F. Cotton (2006a). The nature of noise wavefield and its applications for site effects studies. A literature review, Earth Sci. Rev., 79 (3-4), 205-227.

Bonnefoy-Claudet, S., C. Cornou, P.-Y. Bard, F. Cotton, P. Moczo, J. Kristek and D. Fäh (2006b). H/V ratio: a tool for site effects evaluation. Results from 1D noise simulations, Geophys. J. Int., 167, 827-837.

Bouckovalas, G.D., and G.P. Kouretzis (2001). Stiff soil amplification effects in the 7 September 1999 Athens (Greece) earthquake, Soil Dyn. Earthq. Eng., 21, 671-687.

Bowles, J.E. (1982). Foundation Analysis and Design, McGraw-Hill, New York, 816 pp.

Brandenberg, S.J., N. Bellana and T. Shantz (2010). Shear wave velocity as a statistical function of Standard Penetration Test resistance and vertical effective stress at Caltrans Bridge sites, Report No. PEER 2010/03, Pacific Earthq. Eng. Res Center, 75 pp.

Cadet, H., A. Macau, B. Benjumea, F. Bellmunt and S. Figueras (2011). From ambient noise recordings to site effect assessment: The case study of Barcelona microzonation, Soil Dyn. Earthq. Eng., 31 (3), 271-281.

Cadet, H., P.-Y. Bard, A.-M. Duval and E. Bertrand (2012). Site effect assessment using KiK-net data: part 2 - site amplification prediction equation based on f_0 and Vsz, Bull. Earthq. Eng., 10, 451-489 and 491.

Carvalho, A., G. Zonno, G. Franceschina, J.B. Serra and A.C. Costa (2008). Earthquake shaking scenarios for the metropolitan area of Lisbon, Soil Dyn. Earthq. Eng., 28, 347-364.

Castellaro, S., F. Mulargia and P.L. Rossi (2008). Vs30: proxy for seismic amplification?, Seismol. Res. Lett., 79, 540-543.

Castellaro, S., and F. Mulargia (2014). Simplified seismic soil classification: the Vfz matrix, Bull .Earthq. Eng., 12, 735-754.

Chatelain, J.-L., B. Guillier, F. Cara, A.-M. Duval, K. Atakan, P.-Y. Bard and WP02 SESAME Team (2008). Evaluation of the influence of experimental conditions on H/V results from ambient noise recordings, Bull. Earthq. Eng., 6 (1), 33-74.

Chávez-García, F.J., and P.-Y. Bard (1994). Site effects in Mexico City eight years after the September 1985 Michoacàn earthquakes, Soil Dyn. Earthq. Eng., 13, 229-247.

Cóias e Silva, V. (2005). Construction systems used in the reconstruction. The "Gaiola Pombalina" Recent Studies, In: FLAD and Público (eds.), The Great Earthquake of Lisbon, vol I - Overview, 329-374 (in Portuguese).

Costa, A.C., M.L. Sousa and A. Carvalho (2008). Seismic zonation for Portuguese National Annex of Eurocode 8, Proc. 14WCEE (Beijing, China, October 12-17), 8 pp.

Cotter, J.C.B. (1956). The marine Miocene in Lisbon, Comun. Serviços Geológicos de Portugal, XXXVI, Lisbon, 170 pp. (in Portuguese).

Dikmen, U. (2009). Statistical correlations of shear wave velocity and penetration resistance for soils, J. Geophys. Eng., 6, 61-72.

Duval, A.-M., S. Vidal, J.-P. Méneroud, A. Singer, F. De Santis, C. Ramos, G. Romero, R. Rodriguez, A. Pernia, N. Reyes and C. Griman (2001). Caracas, Venezuela, site effect determination with microtremors, Pure Appl. Geophys., 158, 2513-2523.

Estêvão, J.M.C., and C.S. Oliveira (2012). Point and fault rupture stochastic methods for generating simulated accelerograms considering soil effects for structural analysis, Soil Dyn. Earthq. Eng., 43, 329-341.

Fäh, D., E. Rüttener, T. Noack and P. Kruspan (1997). Microzonation of the city of Basel, J. Seismol., 1, 87-102.

Fnais, M., A. Al-Amri, K. Abdelrahman, K. Al-Yousef, O.A. Loni and E.A. Moneim (2014). Assessment of soil-structure resonance in southern Riyadh City, Saudi Arabia, Arab. J. Geosc. (published online).

Freitas, R., M. Alcântara, F. Rodrigues and C. Pedro (2014). Geological and geotechnical characterization in downtown Alcântara (Lisbon) for the Alcântara rail grade separation, Proc. 14th Nat. Congr. Geotechnics - Geotechnics in Infrastructures, Covilhã, Portugal, 20 pp. (in Portuguese).

Fritsche, S., D. Fah, B. Steiner and D. Giardini (2009). Damage field and site effects: multidisciplinary studies of the 1964 earthquake series in Central Switzerland, Nat. Haz., 48, 203-227.

Gallipoli, M.R., A. Masi, M. Mucciarelli, F. Ponzo and M. Vona (2003). Evidence of soil-building resonance, building frequency shift and (maybe) site-city interaction during the 2002 Molise seismic sequence, EGS - AGU - EUG Joint Assembly, Nice (France), abstract #4234.

Geopsy: http://www.geopsy.org/index.html

GeoSIS_Lx Project (2006-2011). Subsurface 3D geological and engineering geological mapping and modelling for urban areas - Lisbon case-study (PTDC/ECM/64167/2006), http://geosislx.cm-lisboa.pt/GEOSIS/geosis_en.html.

Giammarinaro, S., A. Tertulliani, G. Galli and M. Leta (2005). Investigation of surface geology and intensity variability in the Palermo, Italy, urban area after the 6 September 2002 earthquake, B. Seismol. Soc. Am., 95 (6), 2318-2327.

Gosar, A., J. Roser, B.S. Motnikar and P. Zupancic (2010). Microtremor study of site effects and soil-structure resonance in the city of Ljubljana (central Slovenia), Bull. Earthq. Eng. 8, 571-592.

Grünthal, G., ed. (1998). European Macroseismic Scale 1998, Cahiers Centre Europ. Géodyn. Séismol., 15, Luxembourg, 99 pp.

Guillier, B., K. Atakan, K.-L. Chatelain, J. Havskov, M. Ohrnberger, F. Cara, A.-M. Duval, S. Zacharopoulos, P. Teves-Costa and SESAME Team (2008). Influence of instruments on the H/V spectral ratios of ambient vibrations, Bull. Earthq. Eng., 6 (1), 3-31.

Haghshenas, E., P.-Y. Bard, N. Theodulidis and SESAME WP04 Team (2008). Empirical evaluation of microtremor H/V spectral ratio, Bull. Earthq. Eng., 6 (1), 75-108.

Hanumantharao, C., and G.V. Ramana (2008). Dynamic soil properties for microzonation of Delhi, India, J. Earth Syst. Sci., 117, S2, 719-730.

Hartzell, S., L.F. Bonilla and R.A. Williams (2004). Prediction of non-linear soil effects, B. Seismol. Soc. Am., 94 (5), 1609-1629.

Hasancebi, N., and R. Ulusay (2006). Evaluation of site amplification and site period using different methods for an earthquake-prone settlement in Western Turkey, Eng. Geol., 87, 85-104.

Hasancebi, N., and R. Ulusay (2007). Empirical correlations between shear wave velocity and penetration resistance for ground shaking assessments, Bull. Eng. Geol. Environ., 66, 203-213.

Idriss, I.M. (1990). Influence of local site conditions on earthquake ground motions, Proc. 4th US Nat. Conf. Earthq. Eng., 55-57.

Imai, T. (1977). P-and S-wave velocities of the ground in Japan, Proc. 9th Int. Conf. Soil Mechanics Found. Eng., 2, 127-132.

Imai, T., and K. Tonouchi (1982). Correlation of N-value with S-wave velocity and shear modulus, Proc. 2nd Europ. Symp. Penetration Testing, Amsterdam, 57-72.

IPQ (2010). Eurocode 8 - Design of structures for earthquake resistance. Part 1: General rules, seismic actions and rules for buildings, NP - EN 1998-1, Instituto Português da Qualidade (in Portuguese).

Iyisan, R. (1996). Correlations Between Shear Wave Velocity and In-situ Penetration Test Results, Digest, 96, 371-374.

Jafari, M.K., A. Shafiee and S. Razmkhahet (2002). Dynamic properties of fine grained soils in south of Tehran, J. Seism. Earthq. Eng., 4 (1), 25-35.

Kamalian, M., M.K. Jafari, M.R. Ghayamghamian, A. Shafiee, H. Hamzehloo, E. Haghshenas and A. Sohrabi-bidar (2008). Site effect microzonation of Qom, Iran, Eng. Geol., 97, 63-79.

Koçkar, M.K., and H. Akgün (2007). Evaluation of site characterizations and site effects of the Ankara Basin, Turkey, 4th Int. Conf. Earthq. Geotech. Eng., Paper no. 1241, 10 pp.

Kramer, S.L. (1996). Geotechnical Earthquake Engineering. Prentice Hall, New Jersey, 653 pp.

Kwak, D.-Y., C.-G. Jeong, D. Park and S. Park (2008). Comparison of frequency dependent equivalent linear analysis methods, Proc. 14th World Conf. Earthq, Eng., Beijing (China), 8 pp.

Lebrun, B., D. Hatzfeld and P.-Y. Bard (2001). A site effect study in urban area: experimental results in Grenoble (France), Pure Appl. Geophys., 158, 2543-2557.

Lee, S.H. (1990). Regression models of shear wave velocities, J. Chin. Inst. Eng., 13, 519-532.

Lee, V.W., and M.D. Trifunac (2010). Should average shear-wave velocity in the top 30 m of soil be used to describe seismic amplification?, Soil Dyn. Earthq. Eng., 30, 1250-1258.

Lermo, J., and F.J. Chávez-García (1994). Site effect evaluation at Mexico City: dominant period and relative amplification from strong motion and microtremor records, Soil Dyn. Earthq. Eng., 13, 413-423.

LNEC (1998). Determination of the shear and longitudinal waves velocities in Terreiro do Paço station. Proc. 054/73/10516, Work performed for the Lisbon Metropolitan, E.P., National Laboratory of Civil Engineering, Lisbon, 17 pp. (in Portuguese).

Lopes, I. (2005). Small strain characterization of soils. Application of the surface wave method, PhD Thesis, University of Lisbon, 369 pp. (in Portuguese).

Lopes, I., J.A. Santos and I.M. Almeida (2005). Use of surface waves for geotechnical characterization of soft alluvial deposits - the Póvoa de Santa Iria case study, Near Surf. Geophys., 3, 47-56.

Luzi, L., R. Puglia, F. Pacor, M.R. Gallipolo, D. Bindi and M. Mucciarelli (2011). Proposal for a soil classification based on parameters alternative or complementary to Vs30, Bull. Earthq. Eng., 9, 1877-1898.

Maheswari, R.U., A. Boominathan and G.R. Dodagoudar (2010a). Use of surface waves in statistical correlations of shear wave velocity and penetration resistance of Chennai soil, Geotech. Geol. Eng., 28, 119-137.

Maheswari, R.U., A. Boominathan and G.R. Dodagoudar (2010b). Seismic site classification and site period mapping of Chennai City using geophysical and geotechnical data, J. Appl. Geophys., 72 (3), 152-168.

Matildes, R., R. Taborda, I.M. Almeida, C. Pinto and F.T. Jeremias (2010). 3D geological model of Lisbon, Proc. 11th IAEG Congress - Geologically Active, New Zealand, Taylor Williams & Francis Group, London, 2201-2208.

Matildes, R., I.M. Almeida, R. Taborda and F. Marques (2011). The contribution of GeoSIS_Lx database and geoscientific information system to the reconstruction of Lisbon's coastline, Proc. ICS2011, J. Coastal Res., SI 64, 1702-1706.

Maugeri, M., A.L. Simonelli, A. Ferraro, S. Grasso and A. Penna (2011). Recorded ground motion and site effects evaluation for the April 6, 2009 L'Aquila earthquake, Bull. Earthq. Eng., 9, 157-179.

Mendes-Victor, L.A., C.S. Oliveira, I. Pais and P. Teves-Costa (1994). Earthquake damage scenarios in Lisbon for disaster preparedness, In: B.E. Tucker, M. Erdik and C.N. Hwang (eds.), Issues in urban earthquake risk, NATO ASI Series E, Applied Science, vol. 271, Kluwer Academic Press, Dordrecht, 265-289.

Montilla, J.A.P., C.L. Casado and J.H. Romero (2002). Deaggregation in magnitude, distance, and azimuth in the south and west of the Iberian Peninsula, B. Seismol. Soc. Am., 92 (6), 2177-2185.

Moreira, V.S. (1991). Historical seismicity of Portugal Mainland, 2nd revised ed., Rev INMG, Lisbon, 79 pp. (in Portuguese).

Mucciarelli, M., A. Masi, M.R. Gallipoli, P. Harabaglia, M. Vona, F. Ponzo and M. Dolce (2004). Analysis of RC building dynamic response and soil-building resonance based on data recorded during a damaging earthquake (Molise, Italy, 2002), B. Seismol. Soc. Am., 94, 1943-1953.

Mucciarelli, M., and M.R. Gallipoli (2006). Comparison between Vs30 and other estimates of site amplification in Italy, First Europ. Conf. Earthq. Eng. Seism., Geneva, Switzerland, Paper 270, 7 pp.

Nabilah, A.B., and T. Balendra (2012). Seismic hazard analysis for Kuala Lumpur, Malaysia, J. Earthq. Eng., 16, 1076-1094.

Nakamura, Y. (1989). A method for dynamic characteristics estimation of subsurface using ambient noise on the ground surface, Q.R. Railway Tech. Res. Inst., 30, 25-33.

Nakamura, Y. (1996). Real-time information systems for hazards mitigation, Proc. 11WCEE, Acapulco, Mexico, paper 2134, 8 pp.

Nakamura, Y. (2000). Clear identification of fundamental idea of Nakamura's technique and its applications, Proc. 12WCEE, New Zealand, Paper 2656, 8 pp.

Nath, S.K., and K.K.S. Thingbaijam (2011). Assessment of seismic site conditions: a case study from Guwahati City, northeast India, Pure Appl. Geophys., 168, 1645-1668.

Navarro, M., F.J. Sanchez, T. Enomoto, F. Vidal and S. Rubio (2000). Relation between the predominant period of soil and the damage distribution after Mula 1999 earthquake, Proc. 6th Int. Conf. Seism. Zonation, Palm Spring, California, CD-ROM.

Navarro, M., F. Vidal, T. Enomoto, F. Alcala, A. García-Jerez, N. Abeki and F. Luzón (2009). Correlation between site effects and damage distribution observed during moderate earthquakes in SE Spain, Proc. 8th Int. Workshop on Seismic Microzoning and Risk Reduction, Almeria (Spain), 8 pp.

Oliveira, C.S. (2004). Update of databases of natural frequencies of building structures, bridges, viaducts and pedestrian crossings using expeditious in-situ measurements, Proc. Sísmica2004 - 6th Nat. Congr. Seism. Earthq. Eng., Guimarães, Portugal, 575-590 (in Portuguese).

Oliveira, C.S. (2008). Lisbon earthquake scenarios: a review on uncertainties, from earthquake source to vulnerability modelling, Soil Dyn. Earthq. Eng., 28, 890-913.

Oliveira, R., P. Seco e Pinto, V. Rebelo and V. Rodrigues (1997). Geological studies for the design of Vasco da Gama bridge in Lisbon, Proc. 6th Nat. Geotech. Congr., Lisbon, Portugal, (Invited Conference) 34 pp. (in Portuguese).

Pais, J., C. Moniz, J. Cabral, J.L. Cardoso, P. Legoinha, S. Machado, M.A. Morais, C. Lourenço, M.L. Ribeiro, P. Henriques and P. Falé (2006). Geological Map of Portugal 1:50,000, 34-D (Lisboa), Instituto Nacional de Engenharia, Tecnologia e Inovação, Lisbon (in Portuguese).

Pereira de Sousa, F.L. (1909). Effect of the 1775 earthquake in Lisbon buildings, Publ. Obras Públicas e Minas, Tome XL, 283-495 (in Portuguese).

ProShake (n.d.). Ground response analysis program, Version 1.1, User's Manual. EduPro Civil Systems, Inc. Redmond, Washington.

Régnier, J., H. Cadet, L.F. Bonilla, E. Bertrand and J.-F. Semblat (2013). Assessing non-linear behavior of soils in seismic site response: statistical analysis on KiK-net strong-motion data, B. Seismol. Soc. Am., 103 (3), 1750-1770.

Rodrigues, L.F. (1979). Seismic prospecting methods in engineering geology. The significance of the shear wave, Specialist thesis, LNEC (in Portuguese).

Schnabel, P.B., J. Lysmer and H.B. Seed (1972). SHAKE: A computer program for earthquake response analysis of horizontally layered sites, Rep. EERC 72-12, Earthq. Eng. Res. Center, Univ. Calif., Berkeley.

Seed, H.B., and I.M. Idriss (1970). Soil moduli and damping factors for dynamic response analyses, Rep. EERC 70-10, Earthq. Eng. Res. Center, Univ. Calif., Berkeley, 48 pp.

SESAME WP12 (2004). Guidelines for the implementation of the H/V spectral ratio technique on ambient vibrations - Measurements, processing and interpretation. SESAME European research project, Deliverable D23.12., Project No. EVG1-CT-2000-00026 SESAME, 62 pp.; http://sesame-fp5.obs.ujf-grenoble.fr/Delivrables/Del-D23-HV_User_Guidelines.pdf.

Sitharam, T.G. (2010). Technical document on geotechnical/ geophysical investigations for seismic microzonation studies of urban centres in India, Working Group of Experts Geotech. Eng. (WGE-GT), NDMA, 322 pp.

Sousa, M.L., and A.C. Costa (2009). Ground motion scenarios consistent with probabilistic seismic hazard disaggregation analysis. Application to Mainland Portugal, Bull. Earthq. Eng., 7, 127-147; doi:10.1007/s10518-008-9088-z.

Sun, J.L., R. Golesorkhi and H.B. Seed (1988). Dynamic moduli and damping ratios for cohesive soils, Rep. No EERC 88-15, Earthq. Eng. Res. Center, Univ. Calif., Berkeley, 42 pp.

Teves-Costa, P., J.A. Costa Nunes, M.L. Senos, C.S. Oliveira and D. Ramalhete (1995). Predominant frequencies of soil formations in the town of Lisbon using microtremor measurements, Proc. 5th Int. Conf. Seism. Zonation, Nice (France), vol. II, 1683-1690.

Teves-Costa, P., I.M. Almeida and P. Silva (2001). Microzonation of Lisbon: 1-D theoretical approach, Pure Appl. Geophys., 158, 2579-2596.

Teves-Costa, P., and M.L. Senos (2004). Seismic zonation of Angra do Heroísmo using ambient vibrations, Proc. 4th Spanish-Portuguese Ass. Geodesy Geoph., Figueira da Foz (Portugal), 75-76 (in Portuguese).

Theodulidis, N., and P.-Y. Bard (1995). (H/V) spectral ratio and geological conditions: an analysis of strong motion data from Greece and TaiWan (SMART-1), Soil Dyn. Earthq. Eng., 14, 177-197.

Tuladhar, R., F. Yamazaki, P. Warnitchai and J. Saita (2004). Seismic of the greater Bangkok area using microtremor observations, Earthq. Eng. Struct. Dyn., 33, 211-225.

Turner, A.K. (2003). Definition of the modelling technologies, In: M.S. Rosenbaum and A.K. Turner (eds.), Subsurface Conditions, Lecture Notes in Earth Sciences, 99, Springer, 27-40.

Vilanova, S.P., M.A. Ferreira and C.S. Oliveira (2009). PAD-1.0 Portuguese Accelerometer Database, CD-Rom Edition, Seismol. Res. Lett., 80 (5), 839-844.

Vilanova, S.P., J.F.B.D. Fonseca and C.S. Oliveira (2012). Ground-motion models for seismic-hazard assessment in western Iberia: constraints from instrumental data and intensity observations, B. Seismol. Soc. Am., 102 (1), 169-184.

Wair, B.R., J.T. DeJong and T. Shantz (2012). Guidelines for estimation of shear wave velocity profiles, PEER Report 2012/08, Pacific Earthq. Eng. Res. Center, 68 pp.

Yoshida, N., S. Kobayashi, I. Suetomi and K. Miura (2002). Equivalent linear method considering frequency dependent characteristics of stiffness and damping, Soil Dyn. Earthq. Eng., 22 (3), 205-222.

*Corresponding author: Paula Teves-Costa,
Instituto Dom Luiz, Faculdade de Ciências, Universidade de Lisboa, Lisboa, Portugal; email: ptcosta@fc.ul.pt.